The Application of Dissipative Particle Dynamics Simulation Technique to Complex Fluids

Hongxia Guo

State-Key Lab. of Polymer Physics and Chemistry
Institute of Chemistry, Chinese Academy of Sciences

I. Introduction

➢**DPD** : a particle-based mesoscopic simulation technique for complex fluids

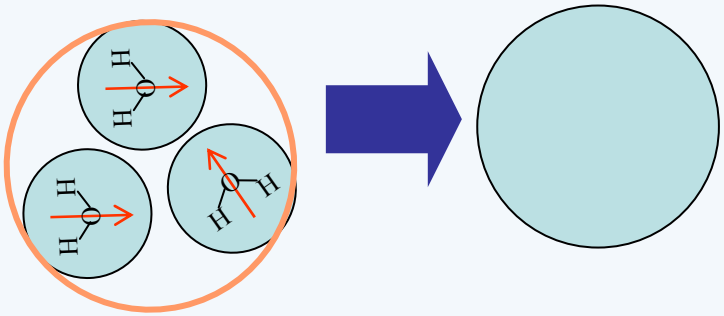

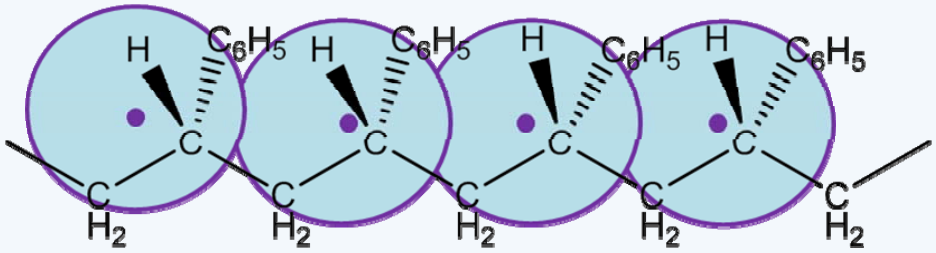

- individual particle represents a cluster of atoms or molecules
- interacts via soft potentials, and is subjected to dissipative and random forces (DPD thermostat)

∴ **DPD simulation a valuable approach over MD and MC**

- DPD thermostat conserves both global and local momentums, is Galilean invariance, avoids profile biasing of NEMD simulation

∴ **DPD thermostat an ideal thermostat in (NE)MD**

II. Application of DPD simulations—1.ternary polymer blends
—2.nanoparticles filled polymer blend
—3. LCs or its related complex systems
--4. lipid

II. Application—1.ternary polymer blends

Interfacial properties and phase transitions in ternary symmetric homopolymerecopolymer blends: DPD

II. Application—1.ternary polymer blends

Polymer blending: an assembly of the interfaces

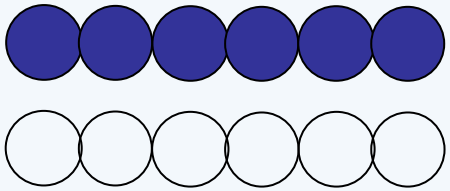

homopolymer A

homopolymer B

macrophase separation

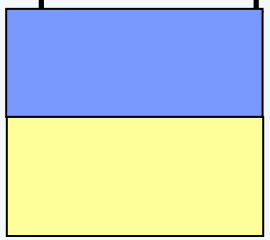

Poor mechanical performance

∴ **compatibilizer-copolymer**

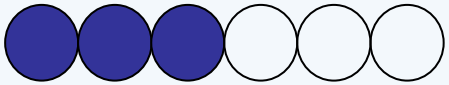

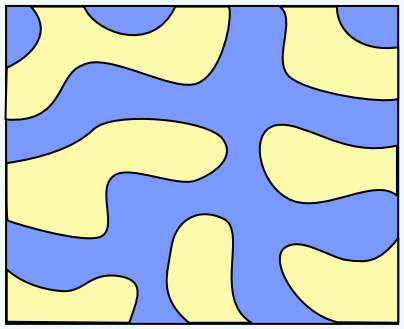

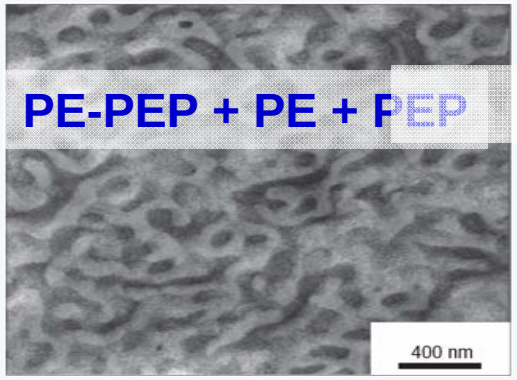

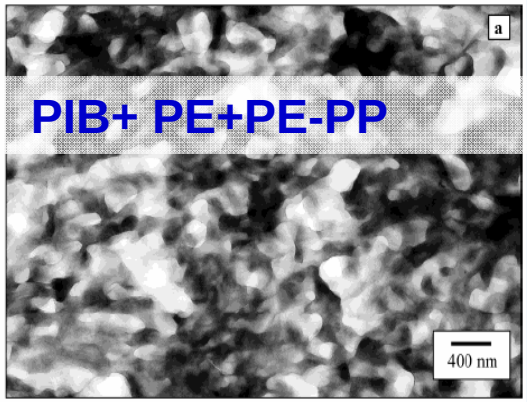

Polymeric microemulsions

Improved mechanical/transport property

Many Applications: **elastomer, porous membranes**

Bates et al. *Phys. Rev Lett.* 1997, 79 849

Macromolecules 2003, 36, 6537-6548; 2004, 37, 7401; 2006, *39*, 1125; 2007, *40*, 355; and 2007, *40*,1207

II. Application—1.ternary polymer blends

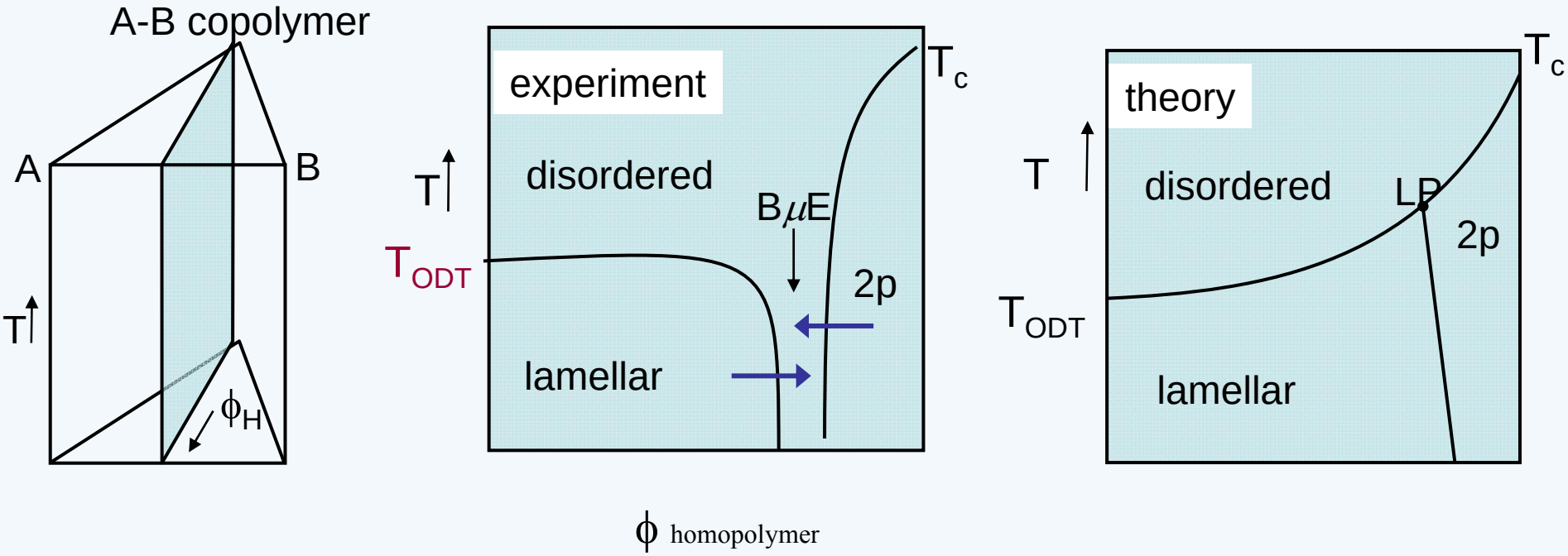

symmetric ternary blend

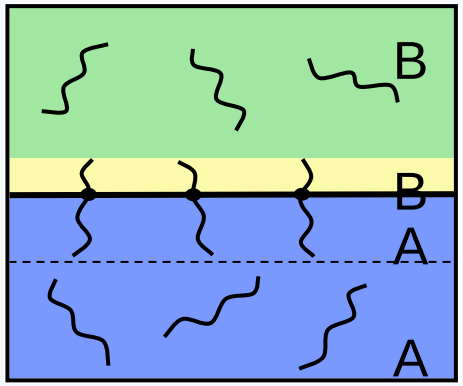

our interest:

- interfacial properties of such blends (especially lamellar phase)
- their relevance to the phase transitions

II. Application—1.ternary polymer blends

Why DPD not MD:

- long-time and metastability in ternary polymer blend
- their phase behavior and interfacial properties within the mesoscopic spatio-temporal scale
- DPD: soft repulsive potential and a momentum conserving thermostat

Interfacial properties: Interfacial tension γ, bending modulus k, interlayer compressibility modulus B

Measurement : the undulation spectrum requires simulations on a relatively large system, as this method is only applicable in the ‘‘long-wavelength’’ limit!!!.

II. Application—1.ternary polymer blends

➢Elasticity of an amphiphilic monolayer between coexisting phases

the undulation spectrum: these interfaces display **long-wavelength fluctuations** = single smoothly undulating surfaces

Helfrich's curvature model:

$$f = \int dA\left[\gamma + \frac{k}{2}(c_1 + c_2 - c_0)^2 + k' c_1 c_2\right] \Longrightarrow f = \int_A dxdy\left[\frac{\gamma}{2}\left(\frac{\partial h}{\partial x} + \frac{\partial h}{\partial y}\right)^2 + \frac{k}{2}\left(\frac{\partial^2 h}{\partial x^2} + \frac{\partial^2 h}{\partial y^2}\right)^2\right]$$

***h*(*x*,*y*):** a height fluctuation function, the displacement of the interface from its mean position

a Fourier transform $f(\tilde{h}_q) = \frac{\gamma}{2} q^2 \tilde{h}_q + \frac{k}{2} q^4 \tilde{h}_q$

equipartition theorem $< f(\tilde{h}_q) >= \frac{1}{A}\frac{K_B T}{2}$

⟹ **spectral intensities of each undulation mode**

$$<|\tilde{h}_q|>= \frac{1}{A}\frac{K_B T}{(\gamma q^2 + k q^4)}$$

⇓

interfacial structure factor

$$S(q) =<|\tilde{h}_q|> A$$

$$\frac{1}{q^2 S(q)} \sim \gamma + k q^2$$

⟸

fitting undulation spectrum **at small q**

interfacial tension γ

bending modulus k

II. Application—1.ternary polymer blends

➢Elasticity of the lamellar phase

Discrete Harmonic：lamellae as a discrete set of two-dimensional fluctuating layers, stacked in the z direction, the energy cost due to local layer deformations and local deviations from the average interlayer distance

$$f = \int dA\left[\gamma + \frac{K_c}{2}(c_1 + c_2 - c_0)^2 + k'c_1c_2\right] \longrightarrow f = \sum_{n=0}^{N-1}\int_A dxdy\left\{\frac{K_c}{2}\left(\frac{\partial^2 h_n}{\partial x^2} + \frac{\partial^2 h_n}{\partial y^2}\right) + \frac{B}{2}\left(h_n - h_{n+1}\right)^2\right\}$$

bending modulus Kc and compressibility modulus B

trans-bilayer structure factor:

$$s_n(q_\perp) = \frac{1}{N^2}\sum_{q_z} e^{iq_z nd} <|h(q_\perp, q_z)|^2> = \frac{1}{N}\sum_{i=0}^{N-1} < h_j(q_\perp)\cdot h_{n+j}(q_\perp)^* >$$

$N \to \infty$

$$s_0(q_\perp) = \frac{L_x L_y k_B T}{K_c q_\perp^4}\left[1 + \frac{4}{\lambda}\right]^{-1/2}$$

$$s_n(q_\perp) = s_0(q_\perp)\left[1 + \frac{\lambda}{2} - \frac{1}{2}\sqrt{\lambda(\lambda+4)}\right]^n$$

$\lambda = (\xi q_\perp)^4$ in-plane correlation length

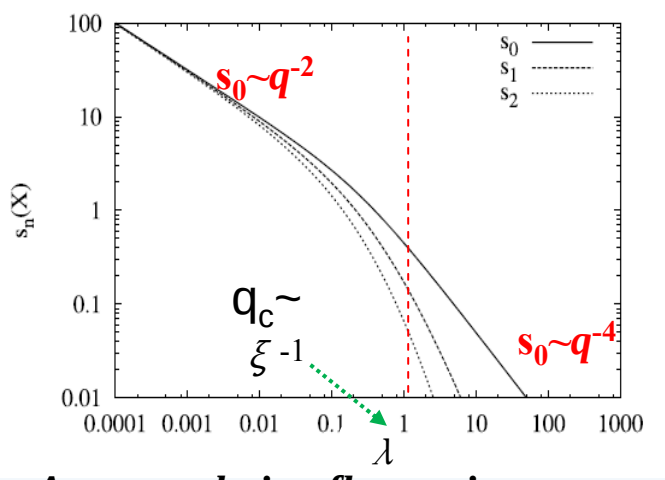

Autocorrelation fluctuation spectra

little work has been done about the undulations and thickness fluctuations in the lamellar phase

II. Application—1.ternary polymer blends

➢Elasticity of lamellar phases

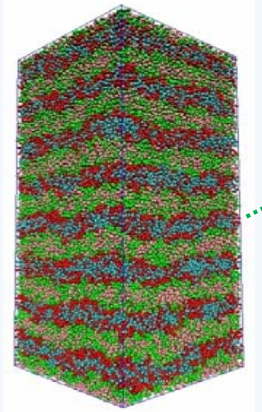

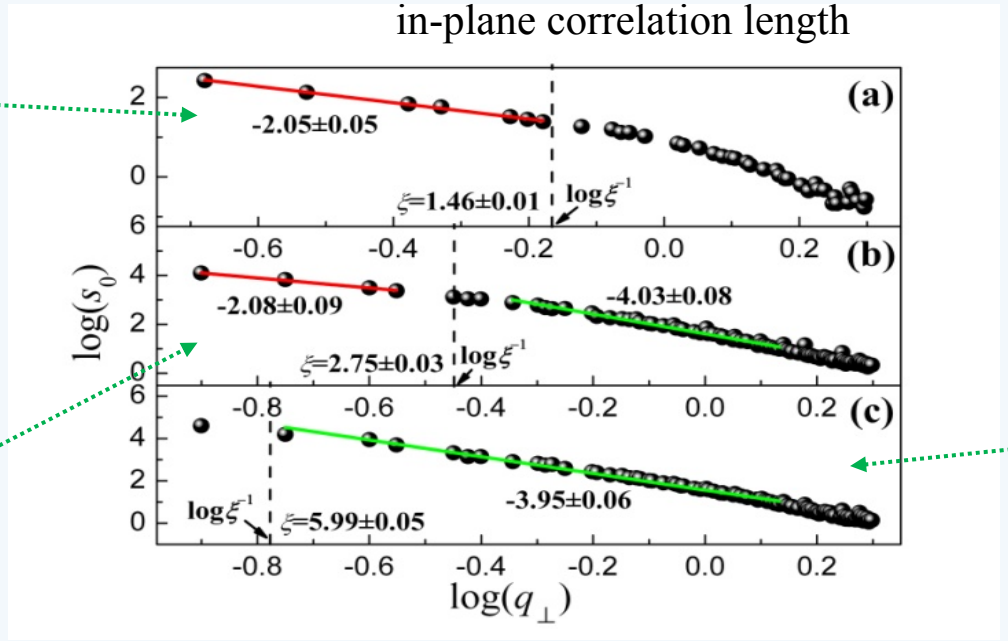

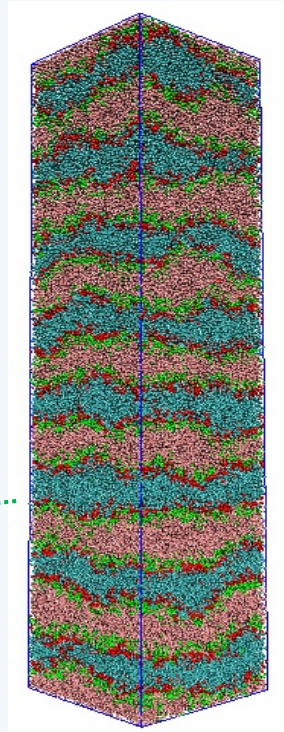

Autocorrelation fluctuation spectra s_0

(a) Φ_H**=0%** , $L_x=L_y=30r_c$, **(b)** Φ_H**=55%** , $L_x=L_y=50r_c$, **(c)** Φ_H**=75%**, $L_x=L_y=50r_c$.

Simulation boxes containing as many as eight lamellae the simulation results can be well compared to the above mentioned continuum theory for stacked membranes.

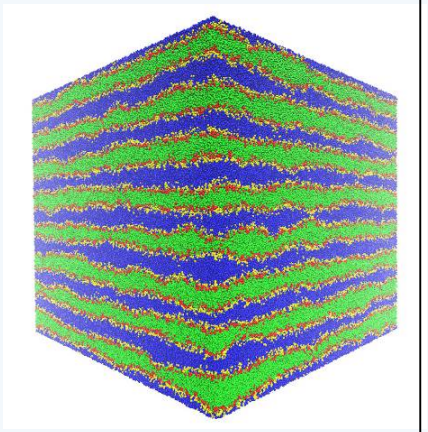

144*144*160

11,059,200 beads! !

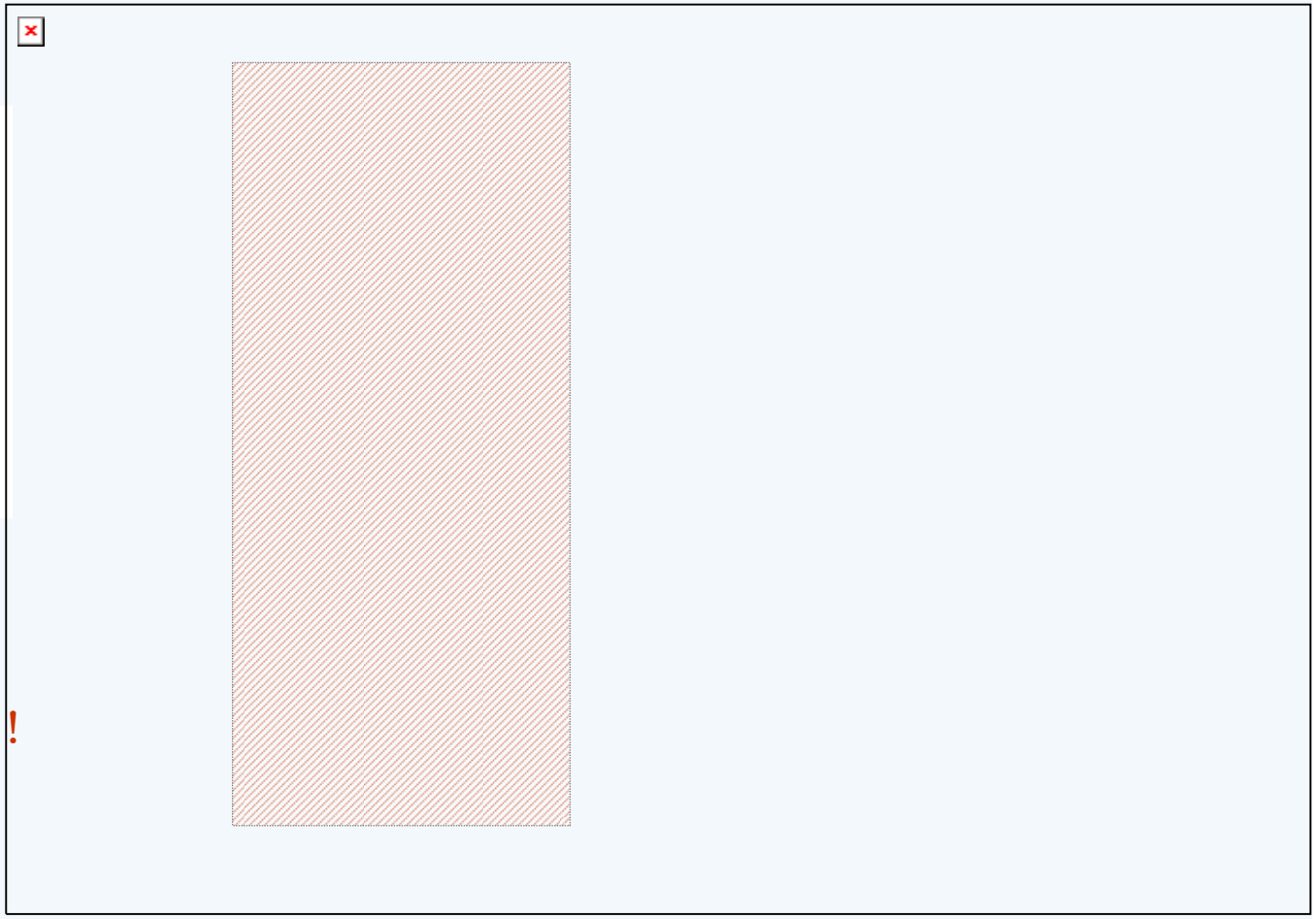

HX GUO, *SOFT MATER.*, **2014**, 12, 2: 185-196

II. Application—1.ternary polymer blends

LAM: lamellar

2P : macro-phase separated phase

DIS: disorder

BuE: bicontinuous microemulsion

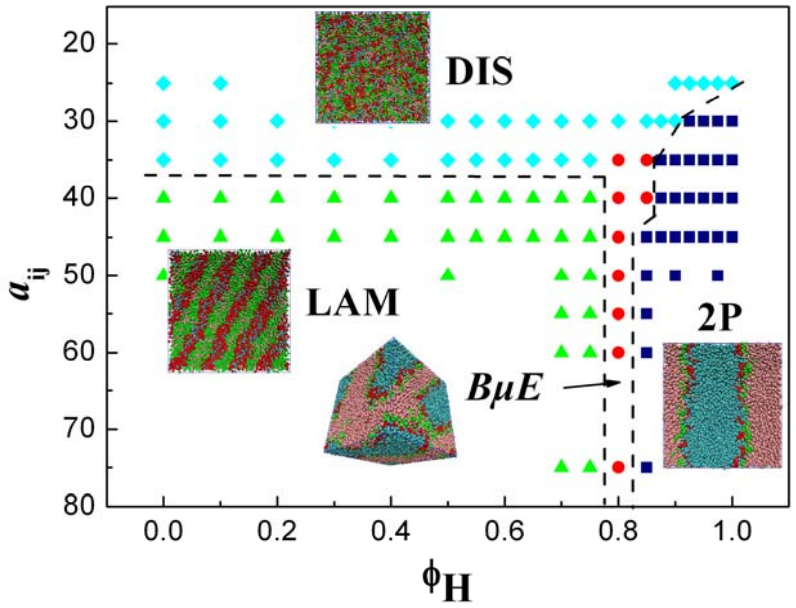

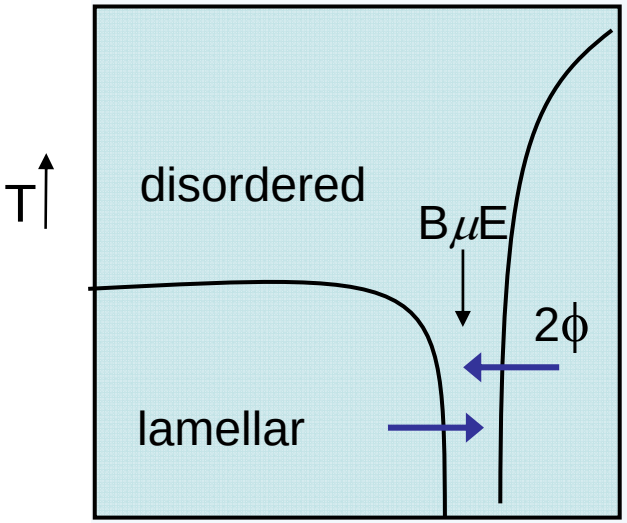

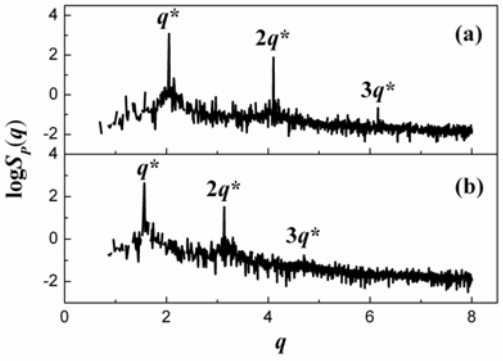

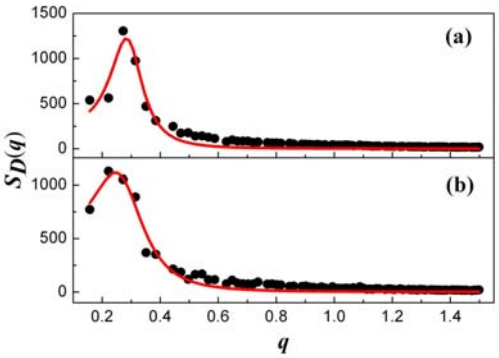

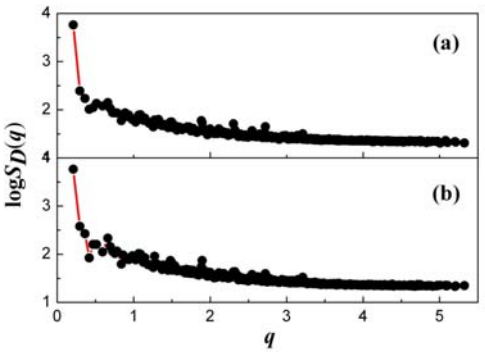

Zhiqiang Bai and HX GUO Polymer, 54:2146-2157(2013)

II. Application—1.ternary polymer blends

- Interfacial properties of 2P phase

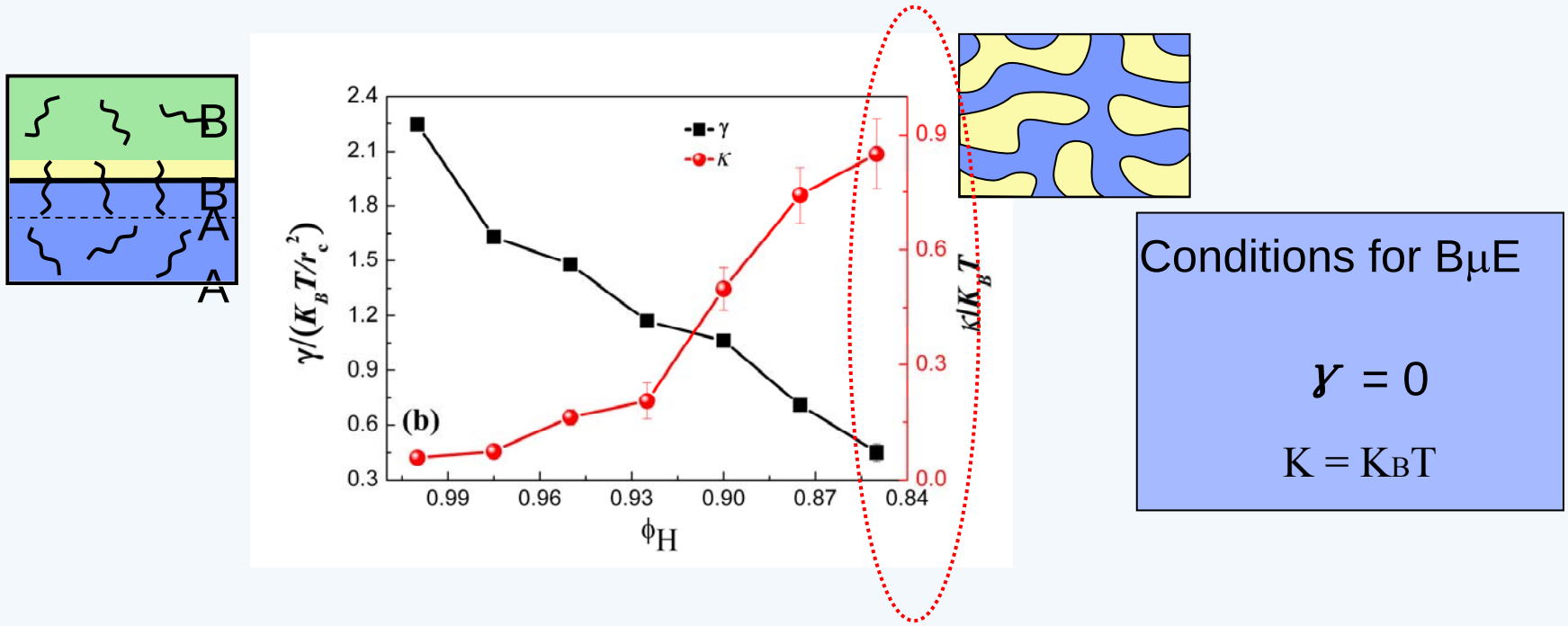

Conditions for BμE

$\gamma = 0$

$K = K_BT$

- γ : BμE structure to accommodate an extensive amount of copolymer-laden internal interfaces
- K: thermal fluctuations to stabilize BμE structure

II. Application—1.ternary polymer blends

- Interfacial properties of LAM phase

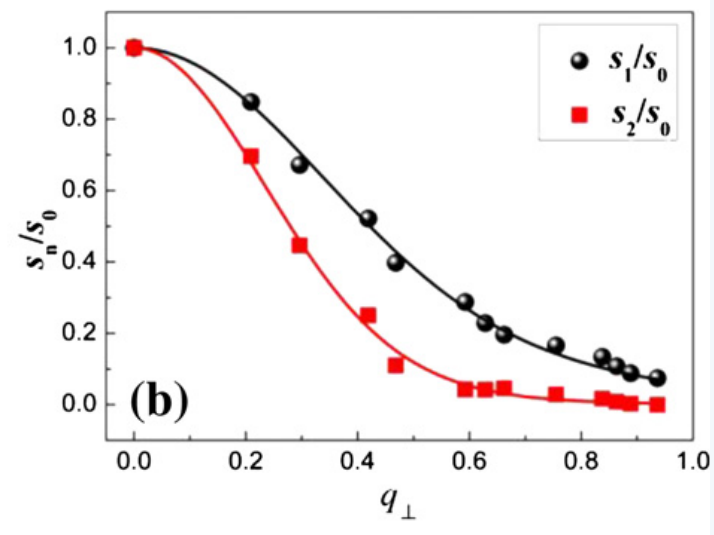

LAM stack of 8 bilayers

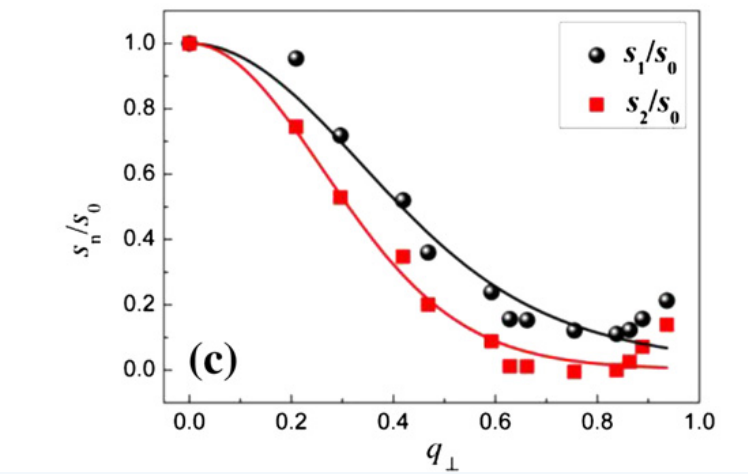

LAM stack of 4 bilayers

Note: DH theory for **an infinitely thick stack of bilayer**

an LAM stack of 8 bilayers is sufficiently large to reproduce the behavior described by continuum DH theory!!!

II. Application—1.ternary polymer blends

- Interfacial properties of LAM phase

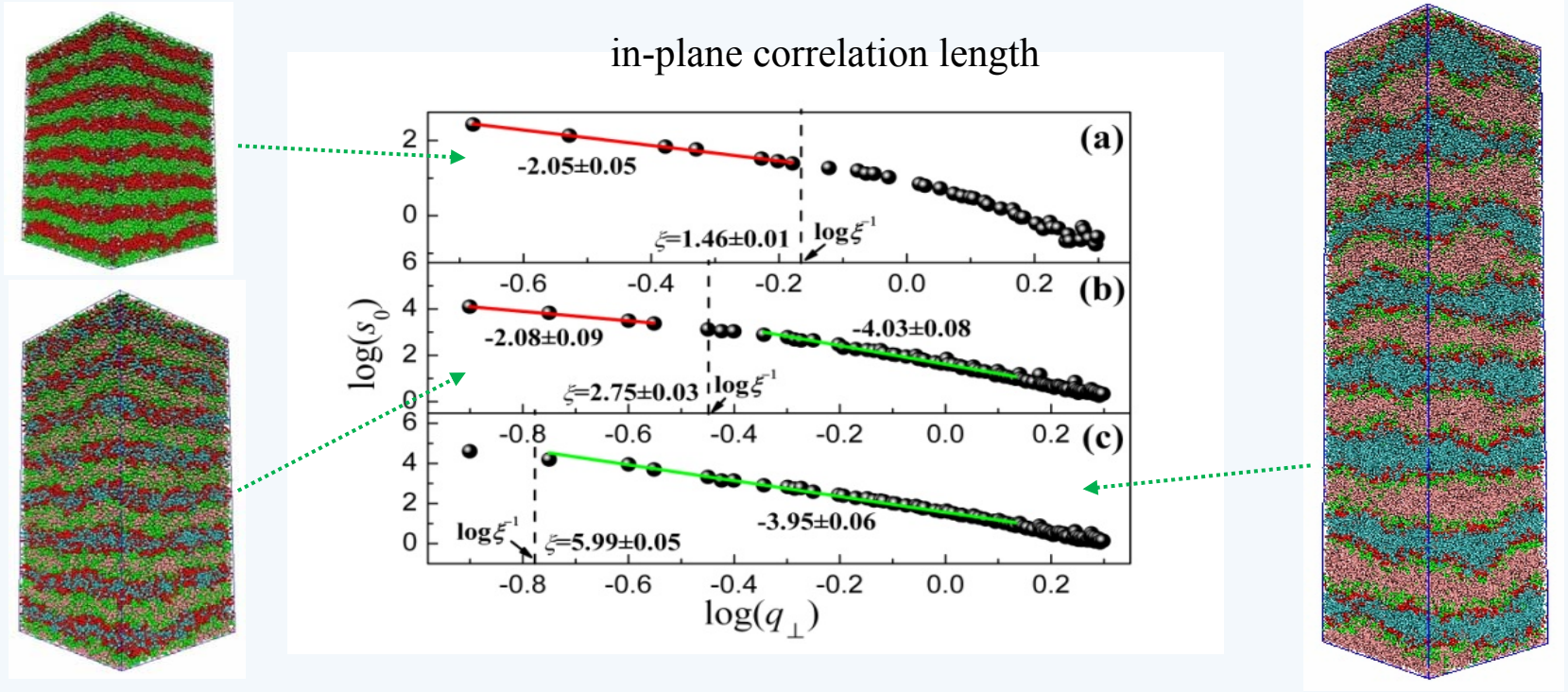

Autocorrelation fluctuation spectra s_0

(a) Φ_H**=0%** , $L_x=L_y=30r_c$, **(b)** Φ_H**=55%** , $L_x=L_y=50r_c$, **(c)** Φ_H**=75%**, $L_x=L_y=50r_c$.

II. Application—1.ternary polymer blends

- Interfacial properties of LAM phase

$$\lambda = a\exp(\frac{2\pi K_c}{K_B T})$$

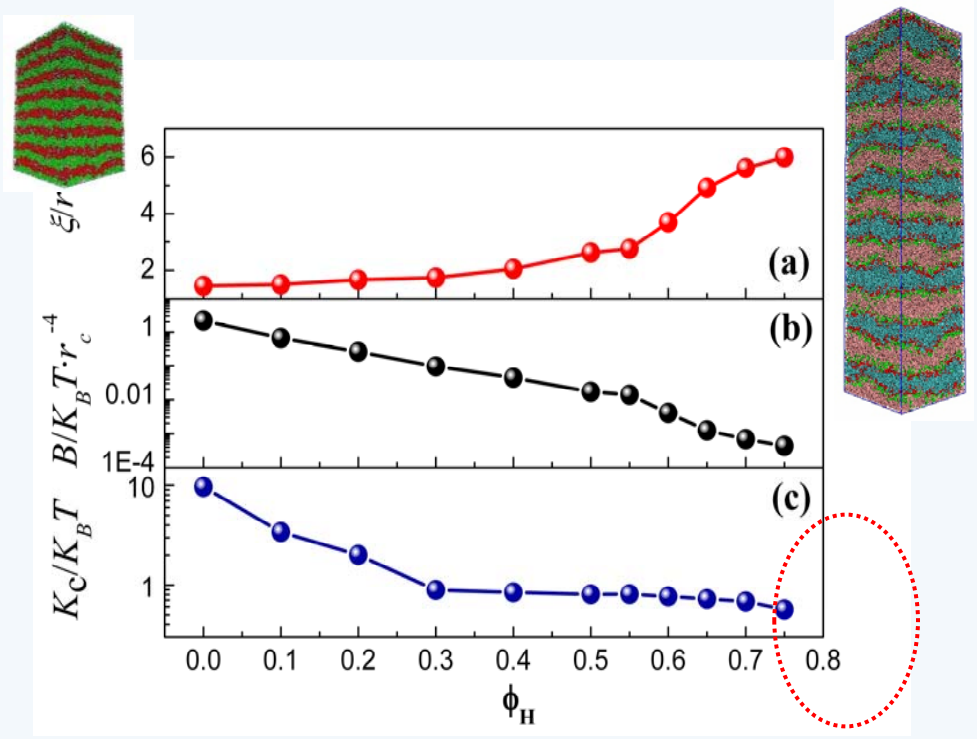

in-plane correlation length ξ
compressibility modulus B
bending modulus ***Kc***
as function of Φ_H

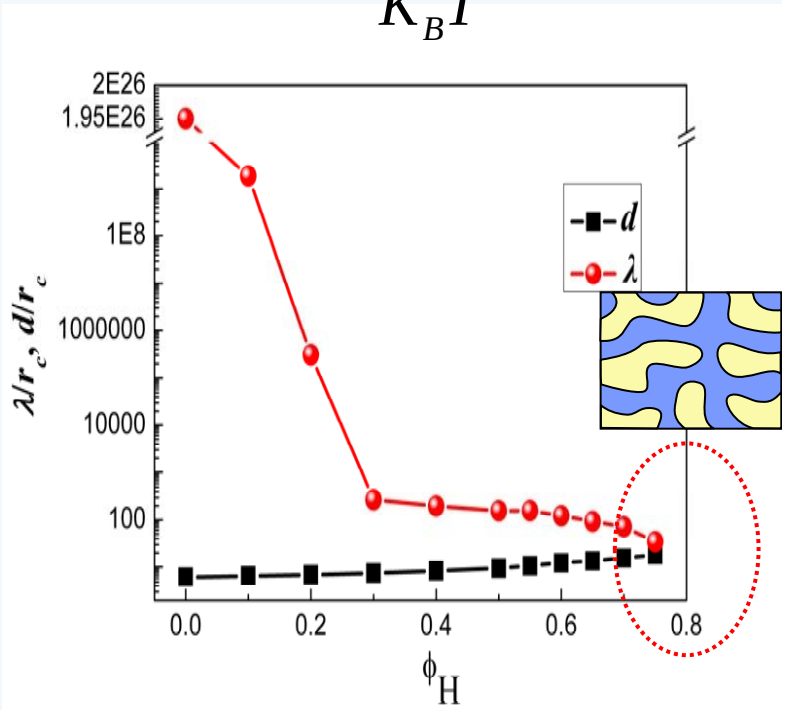

the persistence length of the interface and the lamellar spacing

LAM- BμE: ***Kc<KBT, λ <d***

II. Application—1.ternary polymer blends

- DPD: a simple ternary symmetric system, A4B4/A2/B2
- For the 2P systems:

addition of diblock copolymers, γ reduces but K increases;

phase transition from 2P to BμE: $\gamma = 0$ and $K = K_BT$

- an LAM stack of 8 bilayers is sufficiently large to re-produce the behavior described by continuum DH theory==feasibility of DH theory to calculate Kc and B of the lamellar stack from the simulation data

- For the LAM systems:

with the addition of hompolymers, ξ increases but B and Kc reduce;

phase transition from LAM to BμE :$Kc<K_BT$, $\lambda < d$

fundamental understanding of the interfacial properties and their relevance to the phase transitions in ternary symmetric blends!!

II. Application—2.nanoparticles filled polymer blends

- The effect of Janus nanospheres on the phase separation of polymer blends

- The effect of Janus nanoparticles with various shapes and different dividing surface designs on the ordering and compatibilizing performance in immiscible polymer blends

II. Application—2.nanoparticles filled polymer blends

Nano-particle

unique structural, mechanical, optical, electronic, magnetic properties

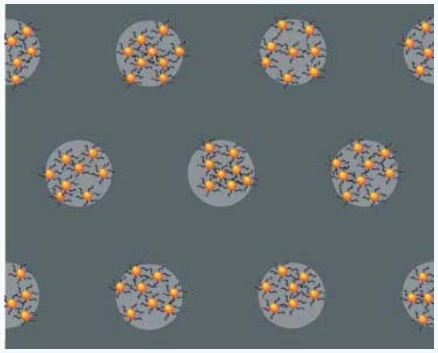

Self-directed self-assembly

Nature 2005, 434, 55

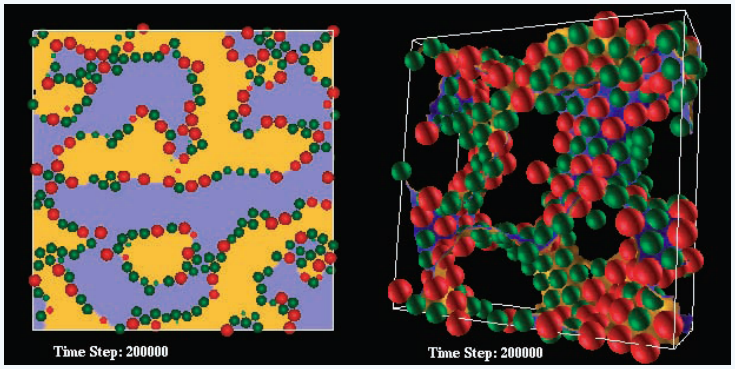

A Route to Fluid-Bicontinuous Gels

Science, 2005, 30,2198

Roman God

=

Janus NP

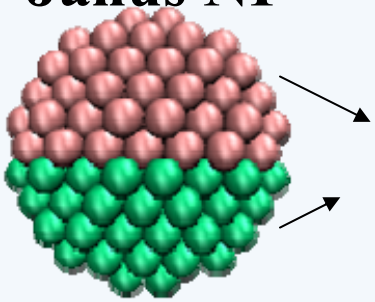

two compartments of
different chemical makeup or surface properties
i.e., hydrophilic hydrophobic

Adv. Mater., 2006, 18, 1152; 2010,22,1060;……

a novel type of efficient stabilizers in polymer alloys

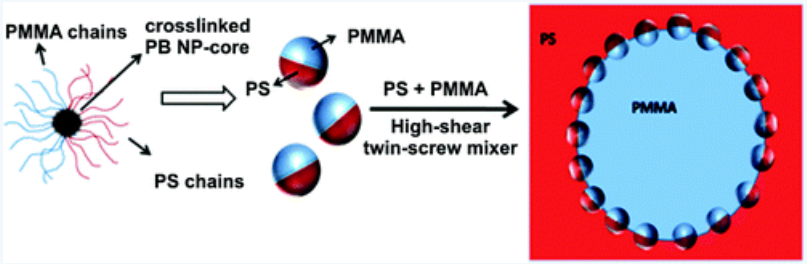

combination of amphiphilicity with the particle character

Or Janus NP as ‘‘solid surfactants’’ to stabilize emulsions and foams

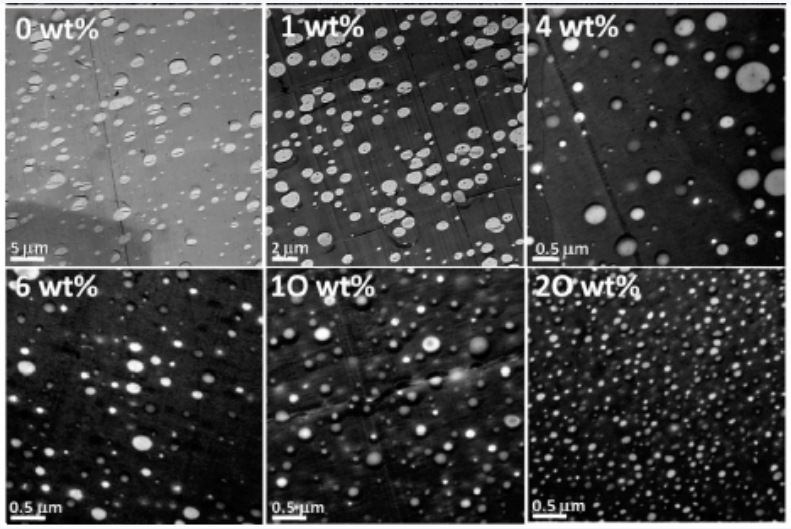

SEM images obtained for blends at a PS/PMMA ratio of 6/4 with Different NP content

Janus nanospheres are superior to block copolymers in the emulsification of the polymer blends

ACS Nano., 2008，2, 1167

Janus NPs : a unique type of building blocks for directional self-assembly of superstructures

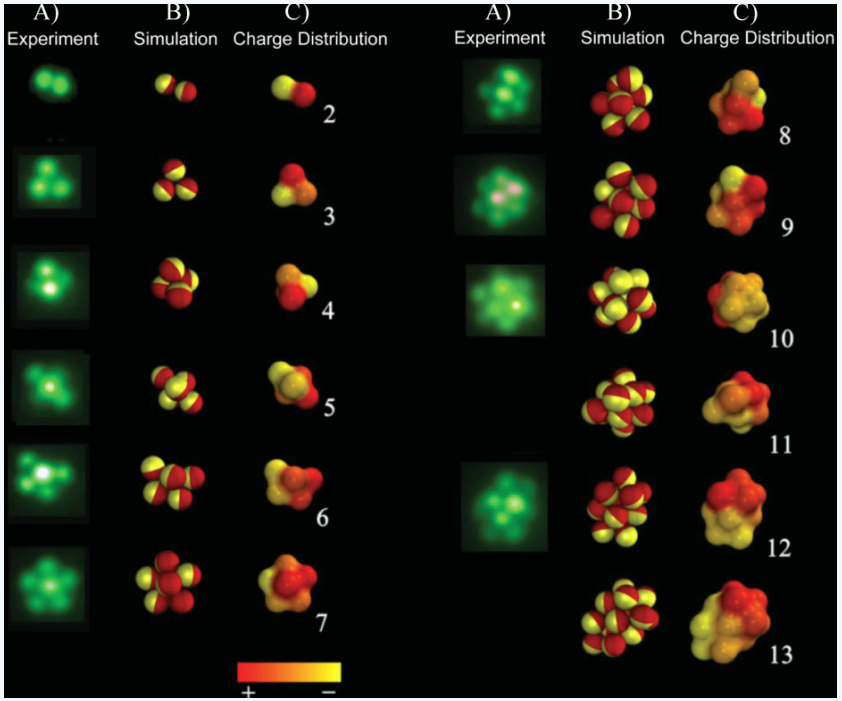

Janus nanospheres in water

complex clusters with various sizes and shapes

Adv. Mater., 2010, 22, 1060

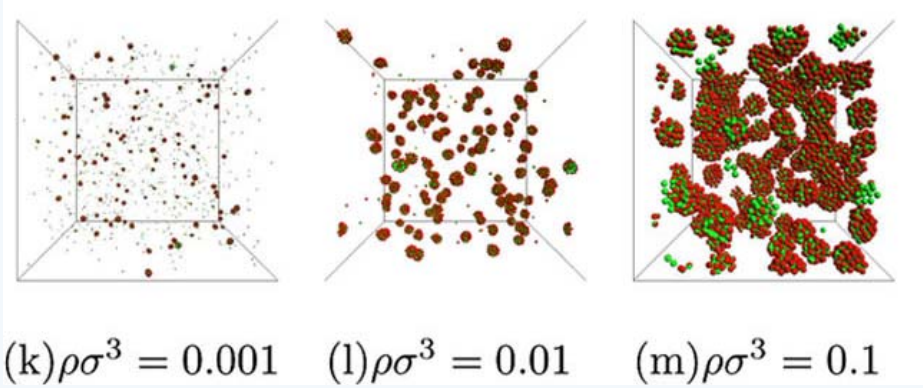

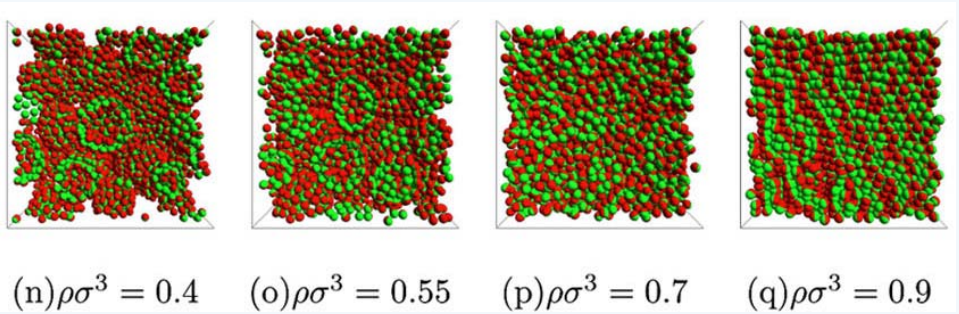

Janus nanospheres in the bulk state

Phys. Rev. Lett., 2009, 103, 237801

the shape of Janus particles: an important design parameter to create self-assembled superstructures

nematic

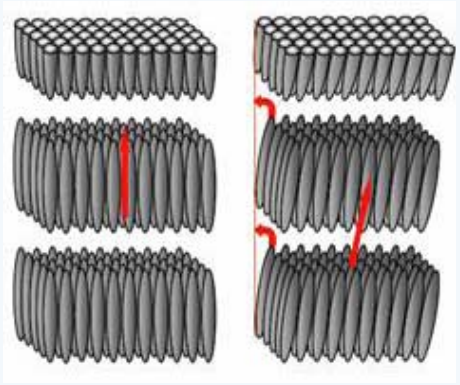

smectic

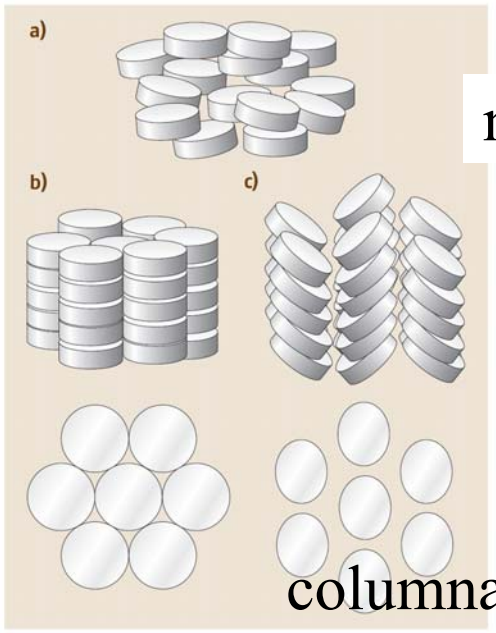

nematic

columnar phase

smectic and columnar phases: internal phase transitions, 2D ordering with a hexagonal or rectangular symmetry within each smectic layer or in the plane orthogonal to columns

non-spherical JNs: Janus character+orientational and positional ordering

complex superstructures and richer mesophases!!!

II. Application—2.nanoparticles filled polymer blends

- The effect of Janus nanospheres on the phase separation of polymer blends

- The effect of Janus nanoparticles with various shapes and different dividing surface designs on the ordering and compatibilizing performance in immiscible polymer blends

Why DPD not MD:

- long-time and metastability in ternary polymer blend
- their phase behavior within the mesoscopic spatio-temporal scale
- DPD: soft repulsive potential and a momentum conserving thermostat

The effect of Janus nanospheres on the phase separation of polymer blends

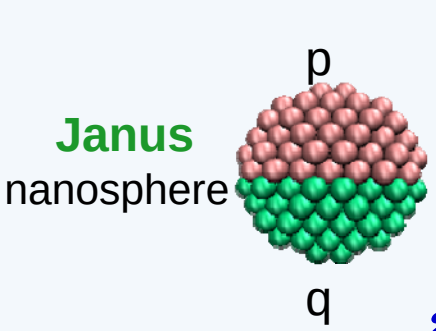

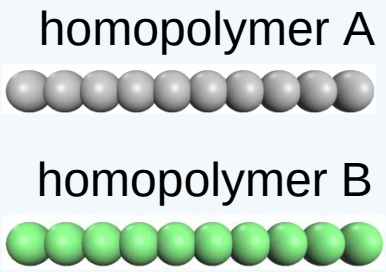

reference system:

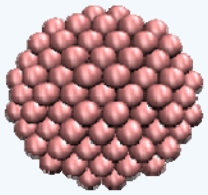

Homogeneous nanosphere with attractions to two homopolymers

a nano-sized microemulsion-like phase

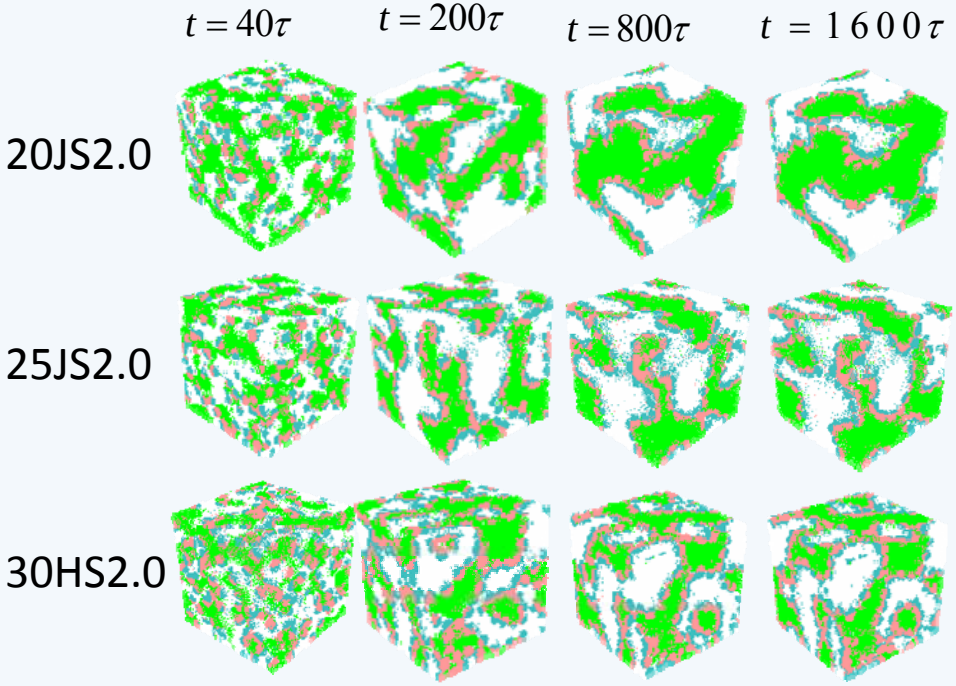

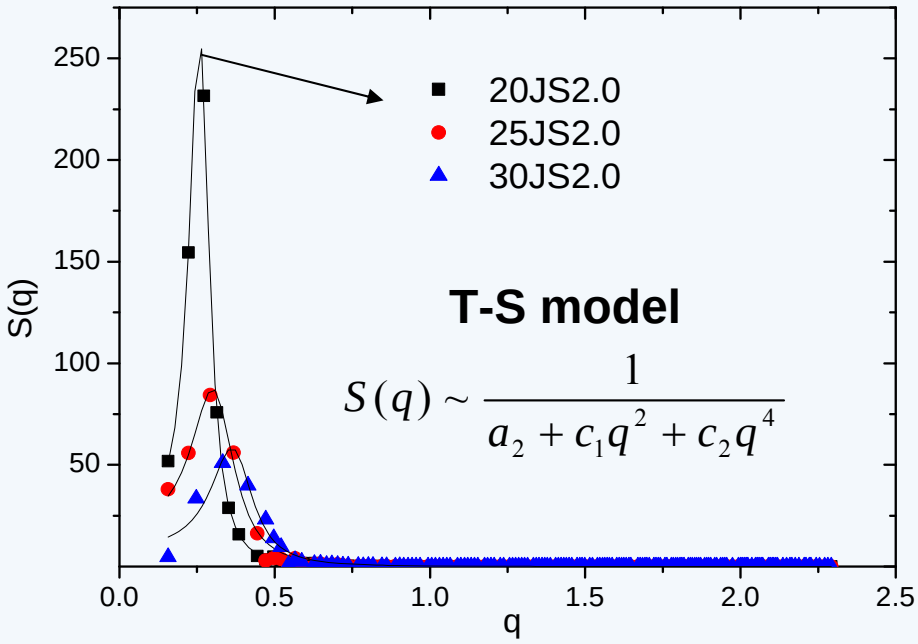

M. Huang, Z. Li and H. Guo, *Soft Matter*, 2012, 8, 6834 – 6845

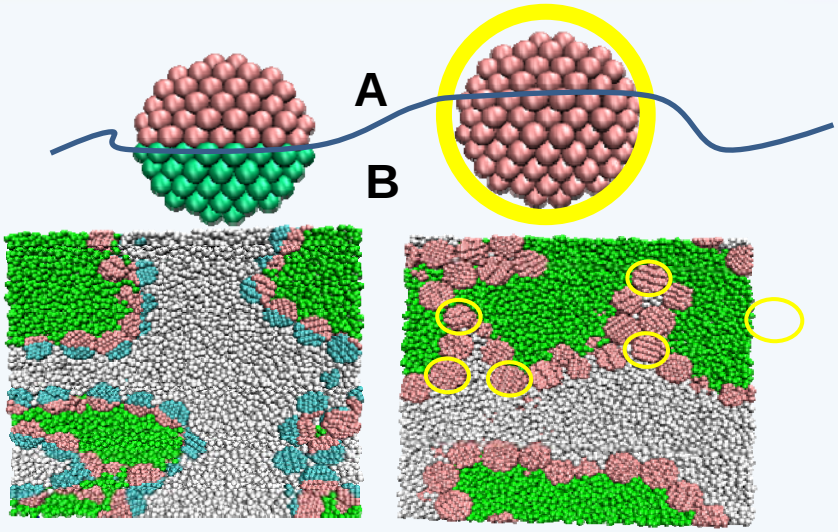

Slowing –down kinetics :

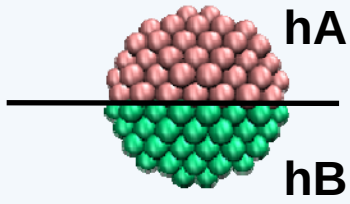

Assumption:

1. adsorbed equatorially

2. no desorption

- equatorial adsorption
- low desorption probability

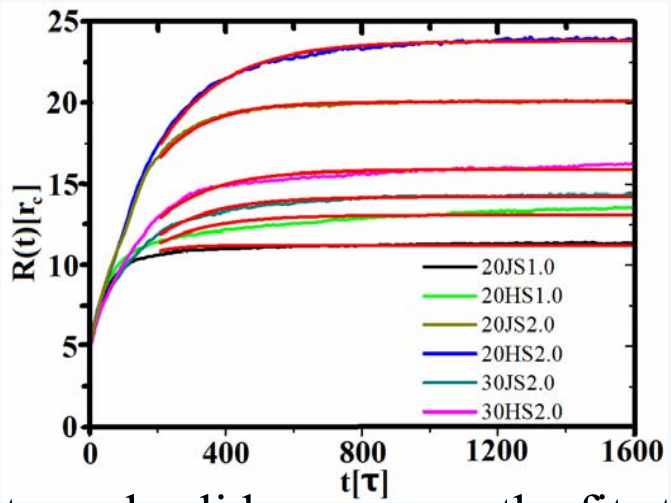

20HS1.0
20JS1.0

20HS2.0
20JS2.0

30HS2.0
30JS2.0

Note: red solid curves are the fits to R(t) using eqn (3) for t > 200s

Model H $\frac{dR(t)}{dt} = \frac{\gamma}{\eta}$

$$R(t) = \frac{\alpha R_{NS}}{\phi_{NS}} - \left(\frac{\alpha R_{NS}}{\varphi_{NS}} - R_0\right)e^{-t/\tau} \quad (1)$$

$$\tau = (\alpha \eta R_{NS})/\gamma_{AB}\phi_{NS}$$

$$t \to \infty \qquad R_{sat} \sim \alpha \frac{R_{NS}}{\phi_{NS}} \quad (2)$$

$$R(t) = R_{sat} - (R_{sat} - R_0)e^{-t/\tau} \quad (3)$$

Dynamical scaling

self-similar behavior
at late stage of SD in symmetric binary fluids

⟹ A scaling of the structure factor

$$S(q,t)=[R(t)]^3 F(x)$$
$$x=q/q_2^{1/2}$$

q2 : second moment of structure factor S(q,t)

the time-independent scaling function $F(x)\equiv\frac{L}{\pi}q_2^{3/2}S(q,t)/\sum_{q=0}^{q=q_c}q^2S(q,t)$

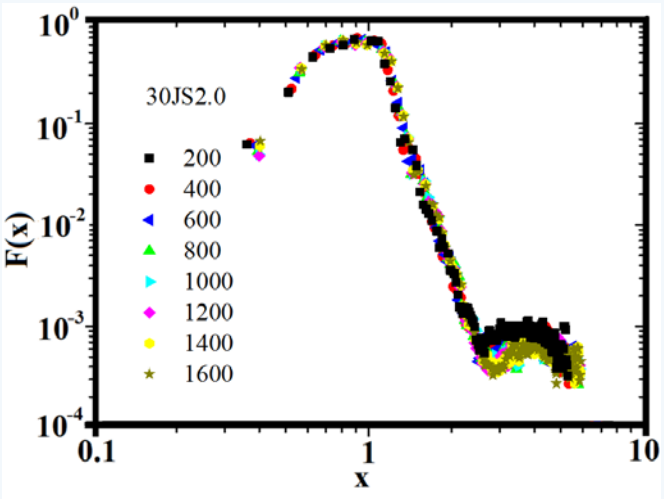

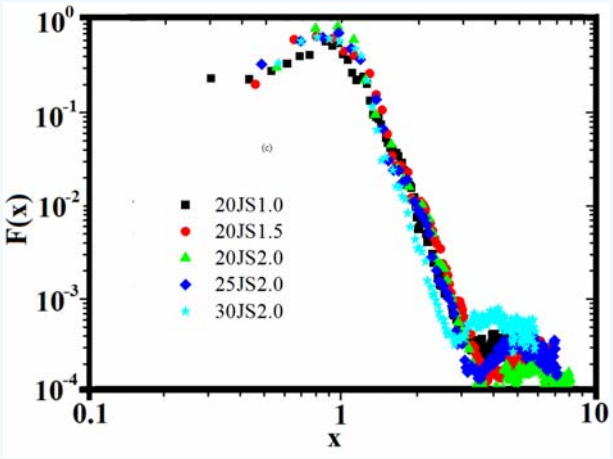

a single characteristic length R(t) can be used to characterize the global morphology evolution and the pattern grows with dynamical self-similarity

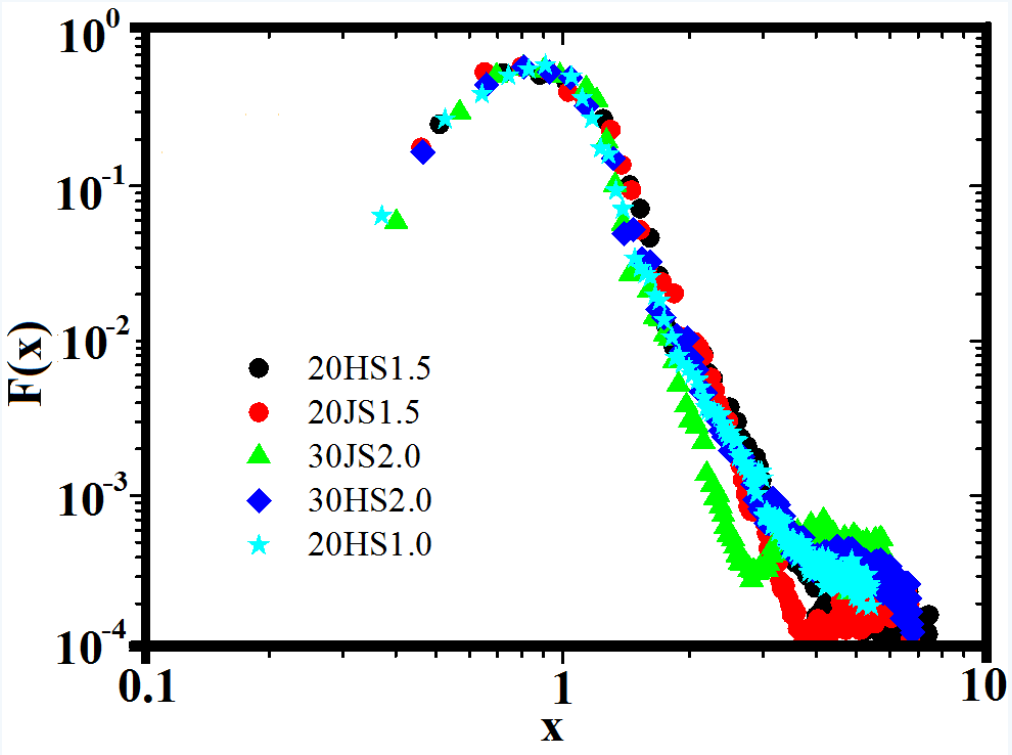

domain growth in the late stage obeys the same mechanism, although the volume fraction, radius, and composition of surface-active nanospheres could alter the growth rate of the phase-separated domains

- **crossover scaling**

for slower late-time phase separation dynamics

linking domain growth **in pure binary polymers** to that in the presence of these surface-active nanospheres

$$R(t) = tf\left(t\phi_{NS}/R_{NS}\right)$$

***f(x)* is the crossover scaling function**

$x = t\phi_{NS}/R_{NS}$ **is the scaling variable**

$x \to \infty \quad f(x) \to x^{-1}$

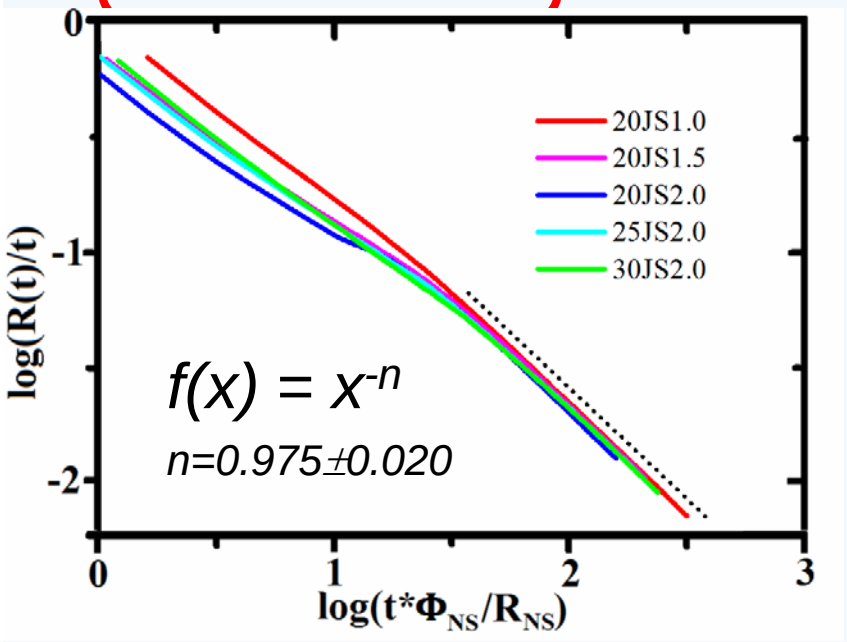

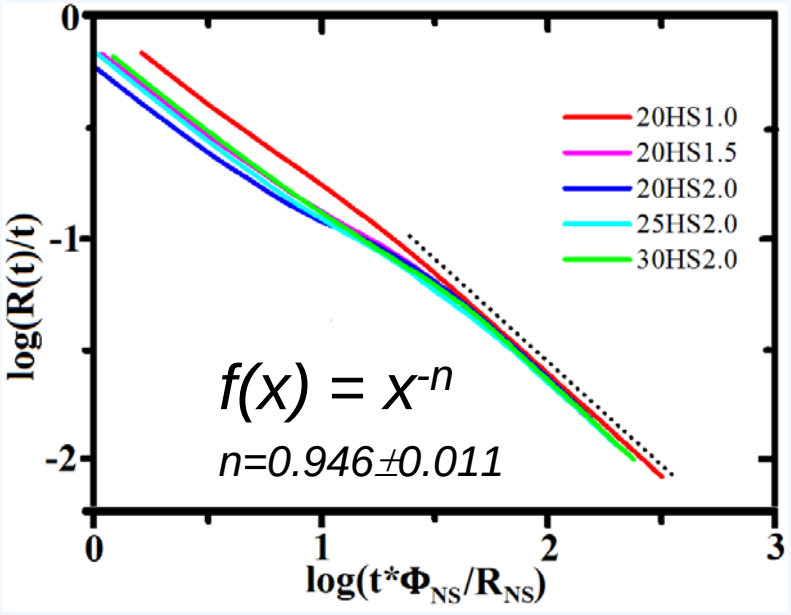

- Due to the inherent equatorial adsorption and low desorption probability Janus nanospheres significantly impede domain growth and at a later stage the average domain size approaches saturation and the growth exponent n decays to near-zero.

- In the later-stage of the phase separation process there exists a dynamical self-similarity in the ternary systems that undergo microphase separation and the domain growth follows a crossover scaling form.

II. Application—2.nanoparticles filled polymer blends

➢**ordering and compatibilizing performance of Janus nanoparticles with various shapes and different dividing surface designs in immiscible polymer blends**

Homopolymer A  Homopolymer B 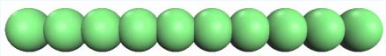

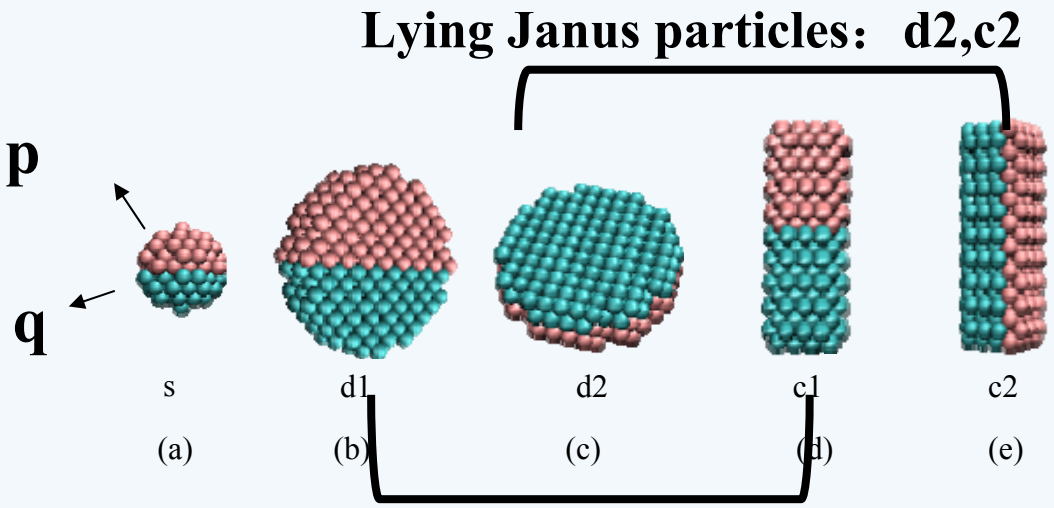

JNs : equal volume fraction and equal net areas

aspect ratios : 2.8 and 0.25

M. Huang and H. Guo, *Soft Matter*, 2013, 9, 7356 – 6845

II. Application—2.nanoparticles filled polymer blends

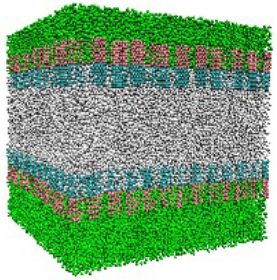

(a) macrophase-separated (2P)state

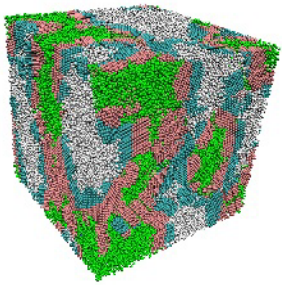

(b) bicontinuous microemulsion-like ($B\,\mu\,E$) phase

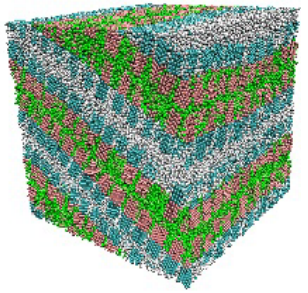

(c) lamellar (LAM) phase

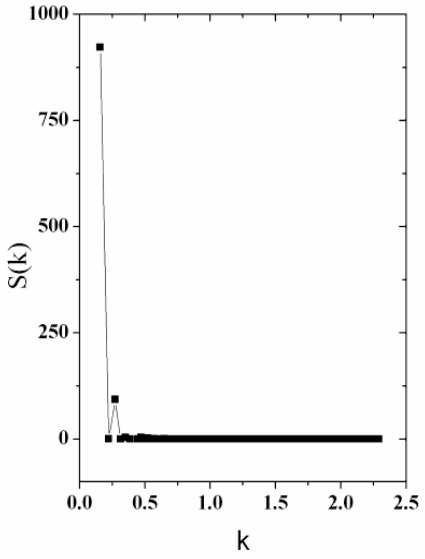

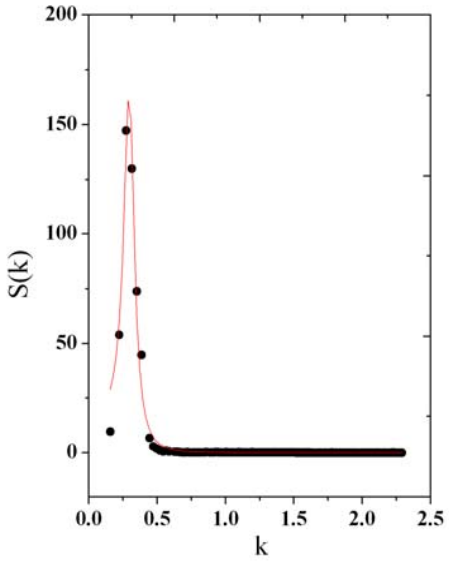

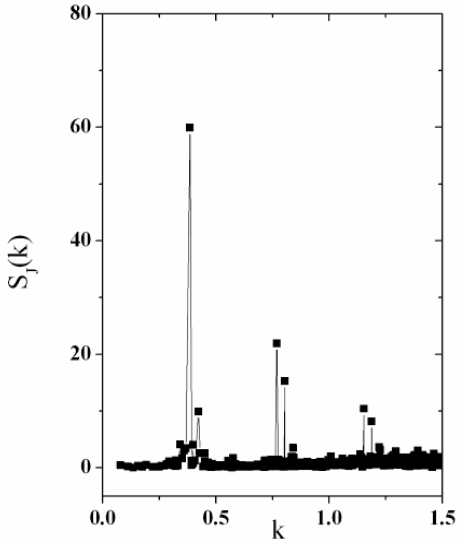

phase diagram

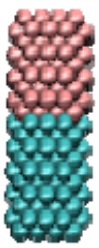

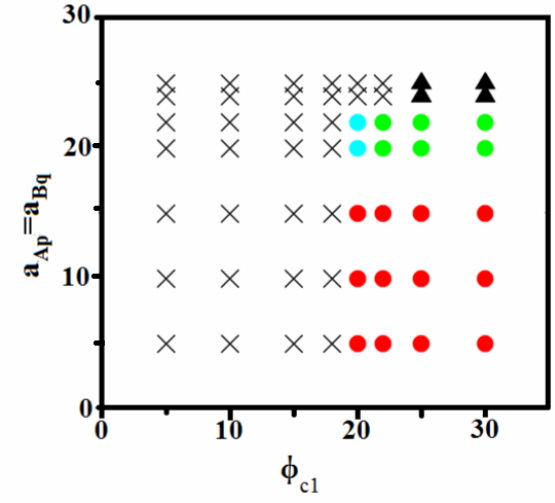

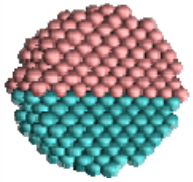

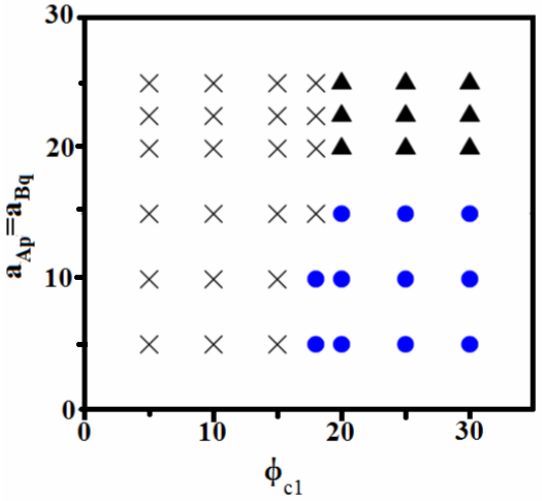

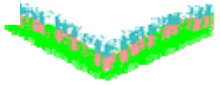

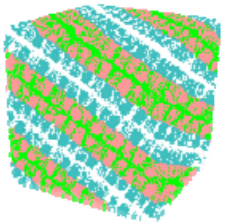

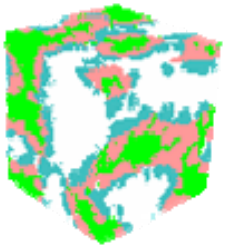

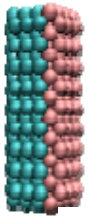

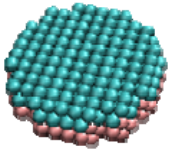

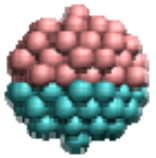

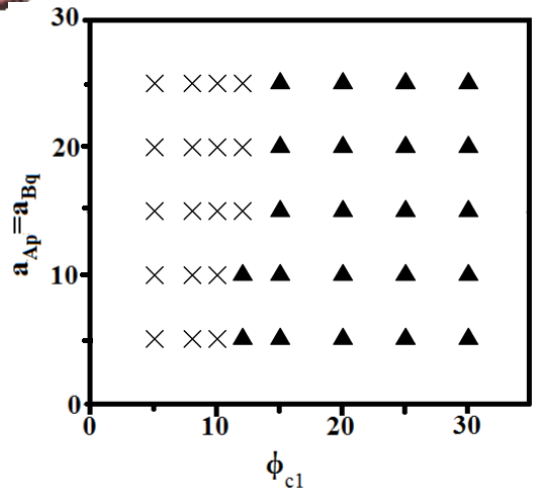

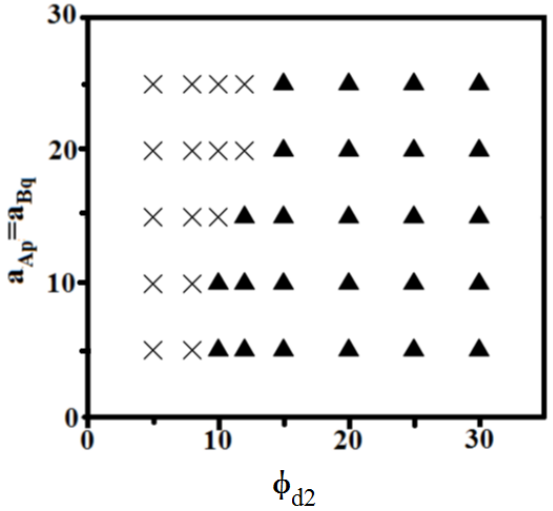

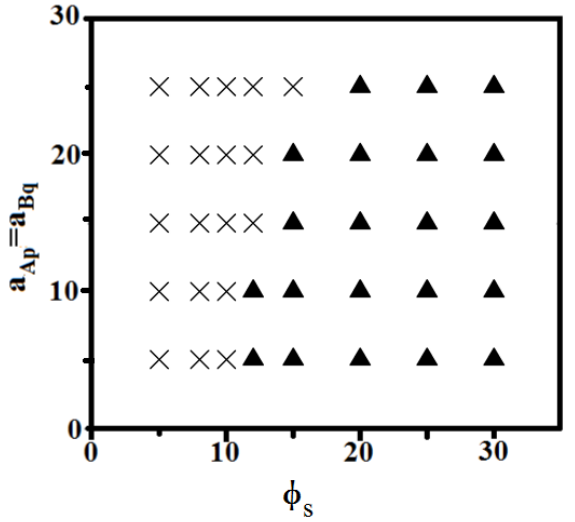

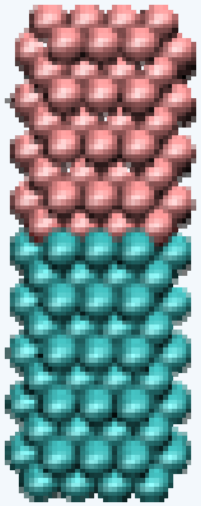

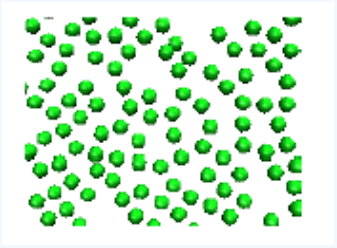

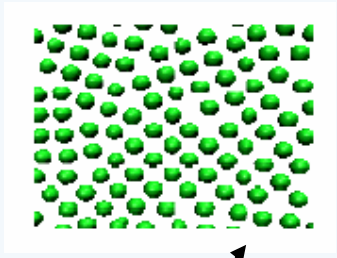

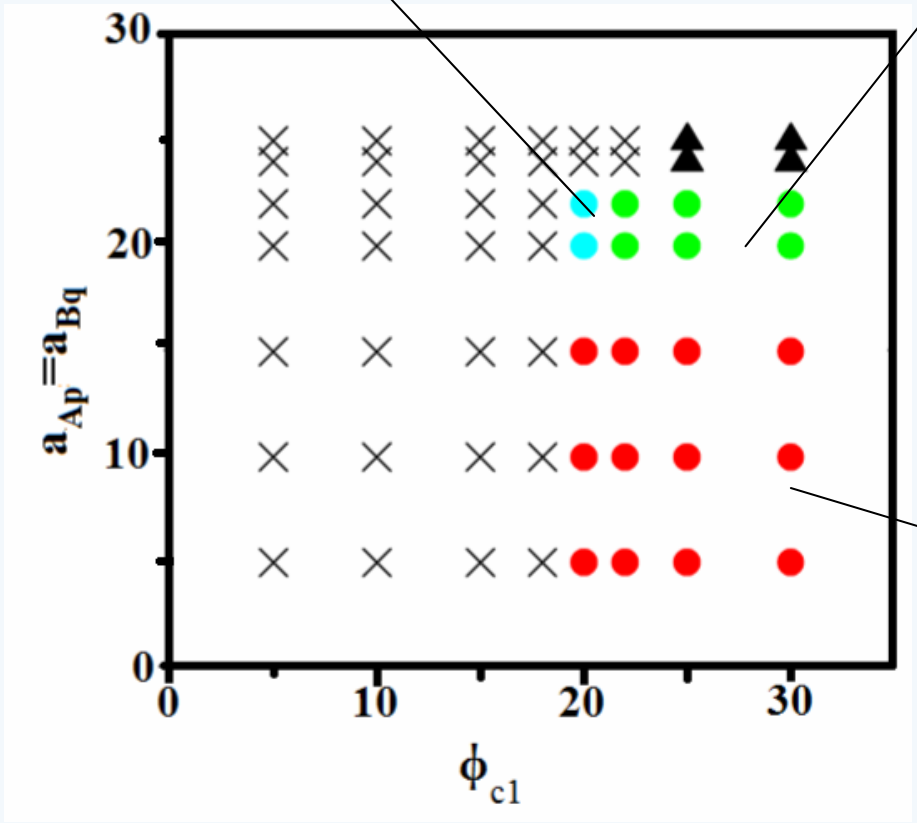
30
20
10
0
0
10
20
30
$a_{Ap}=a_{Bq}$
ϕ_{c1}

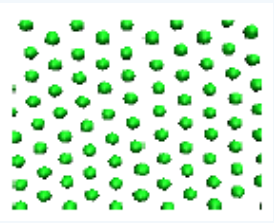

2d-ordering within the layers of the lamellar phase

$1:\sqrt{3}:2$

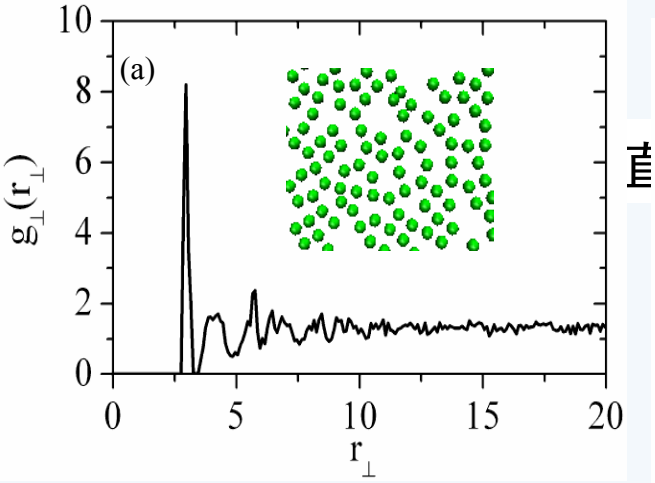

c1-20-20

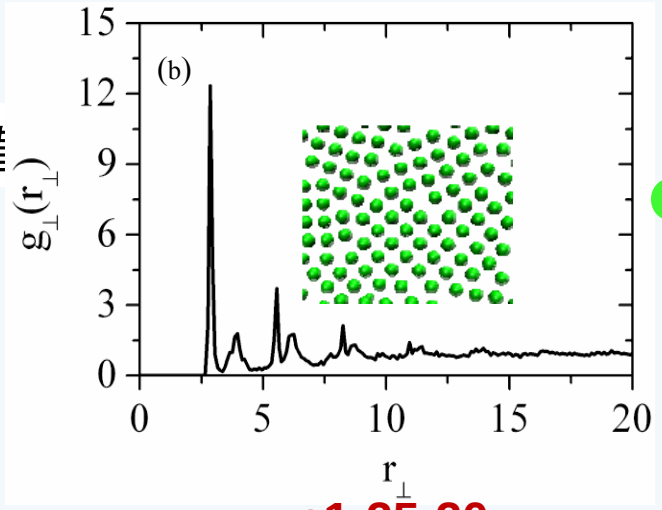

c1-25-20

$1:\sqrt{2}:2$

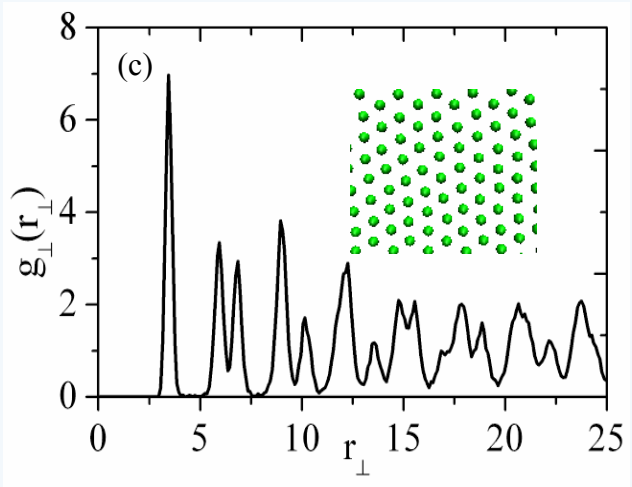

c1-25-15

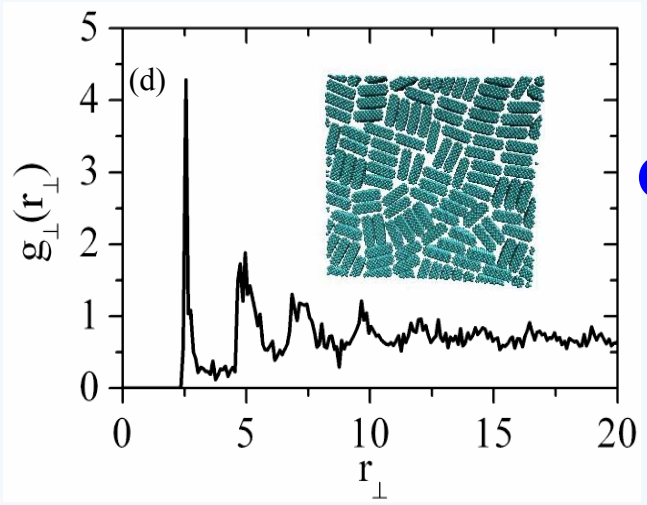

d1-25-10

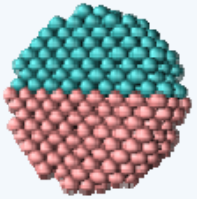

1:2:3

2D radial distribution function for the mass center of particles

local 2d-ordering at the interface layers of the 2P phase

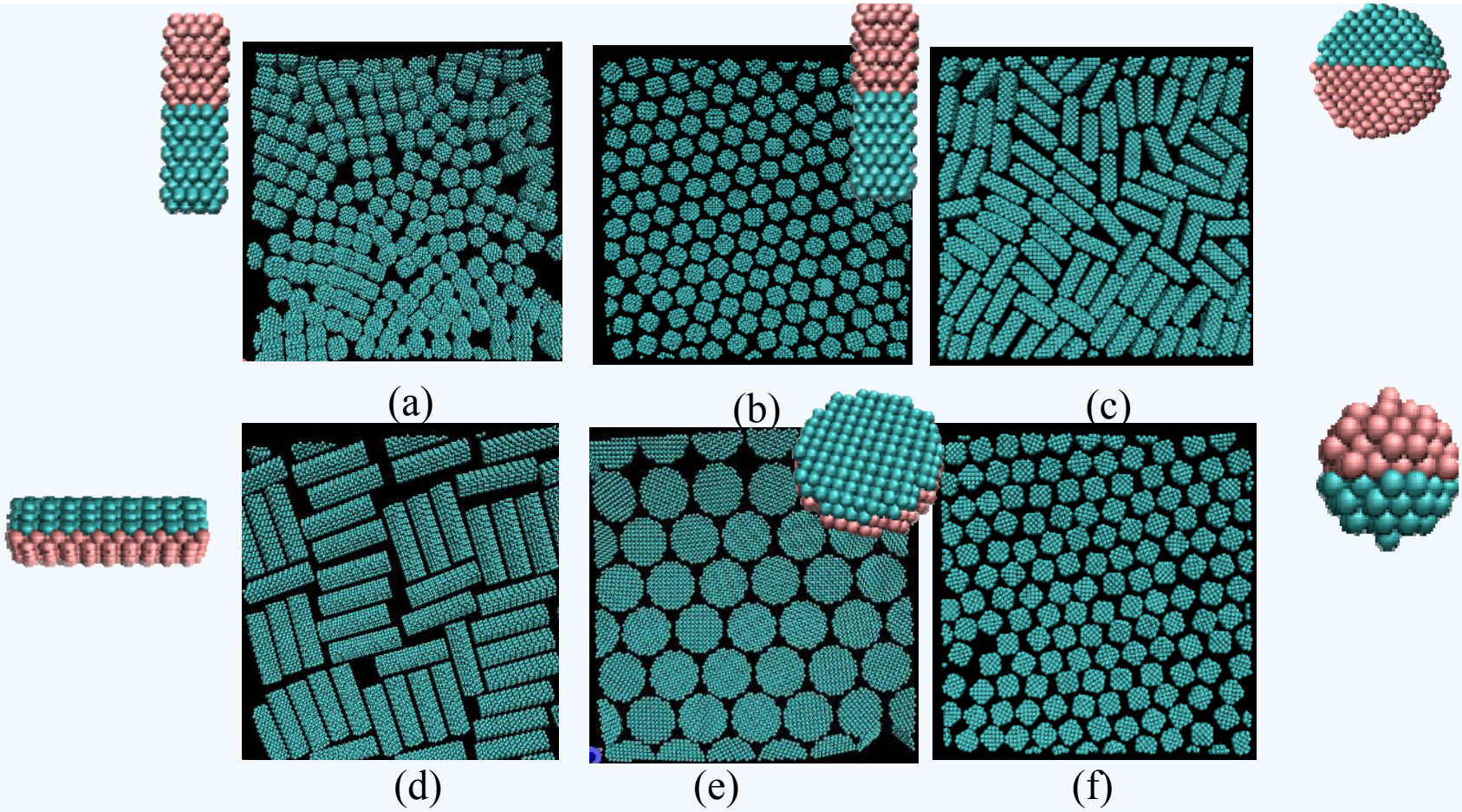

(a) c1-18-20，(b) c1-15-10，(c) d1-10-10，
(d) c2-5-10，(e) d2-5-10 and (f) s-6-10.

Phase separation dynamics

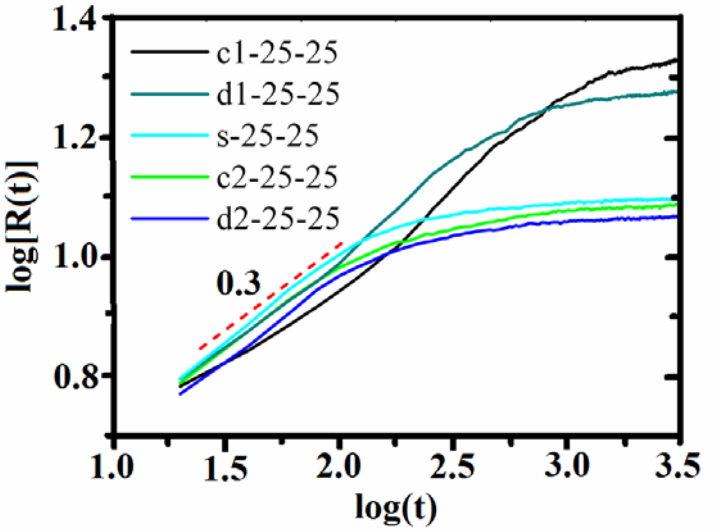

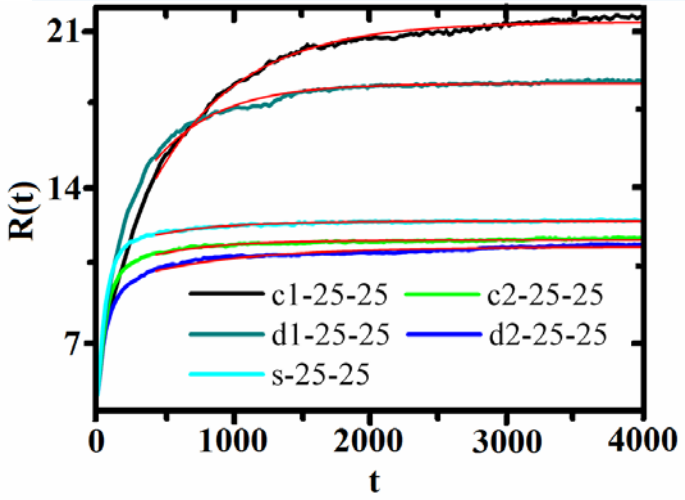

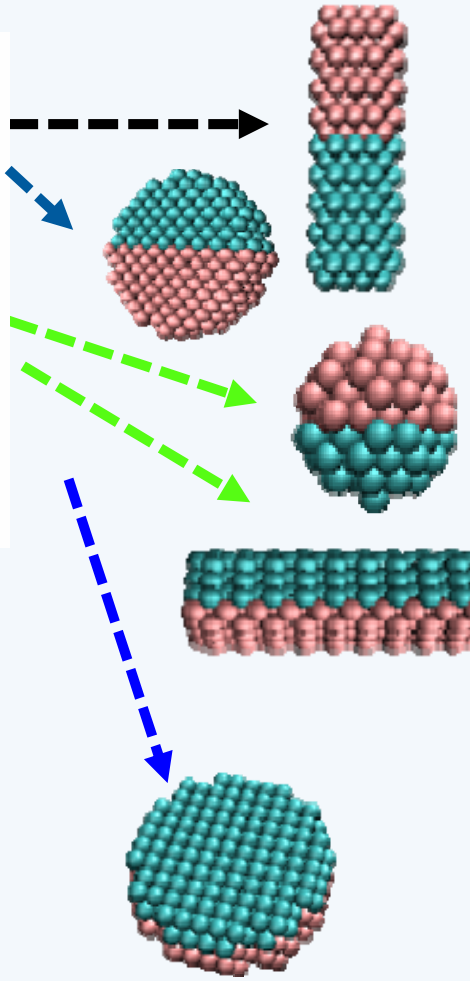

the time-dependent average domain size

at late times $R(t)_{d2} < R(t)_{c2} < R(t)_{s} < R(t)_{d1} < R(t)_{c1}$

System type	c1-25-25	c2-25-25	d1-25-25	d2-25-25	s-25-25
JN type	c1	c2	d1	d2	s
JN number	570	570	398	398	1193
Total dividing surface area of JNs, $A_{tot}(r_c^2)$	2422.5	8800.8	3458.6	10853.5	8136.3
$R_{sat}(r_c)$	21.72	12.21	18.87	11.69	12.63

$$A_{tot}^{d2} > A_{tot}^{c2} > A_{tot}^{s} > A_{tot}^{d1} > A_{tot}^{c1}$$

crossover scaling

$$R(t) \approx tf\left(t/R_{sat}\right)$$

$$x \to \infty \qquad f(x) \to x^{-1}$$

The general mechanism of JNs to stabilize immiscible homopolymers

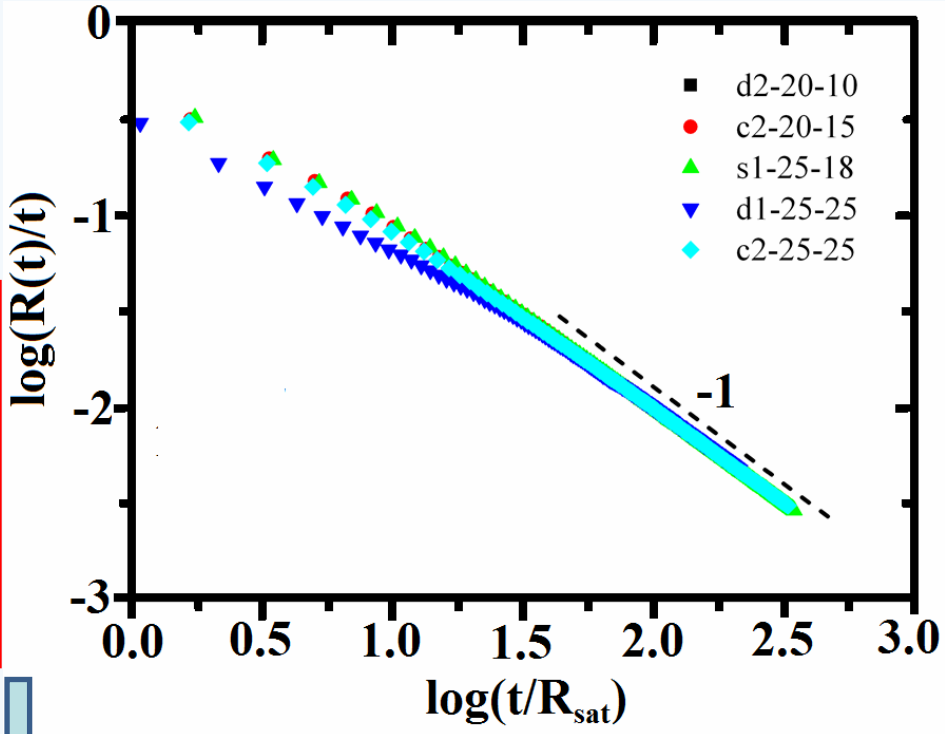

JNs : powerful compatibilizers, greatly reducing the interfacial tension and leading to the formation of bicontinuous microemulsion-like structures

- with the addition of 5%~30% JNs **a BuE structure is observed in all ternary systems while the LAM phase** is only formed in systems **with "standing" anisotropic JNs;**
- lamellar stacks of "standing" JNs assume **several different in-layer structures, which arise from the strong excluded-volume interactions and depend on the particle shape;**
- the addition of JN slows down the phase separation, compatibilizing performance is related to the total dividing surface area of JN which is determined by the particle shapes and dividing surface designs.
- domain growth dynamics at the late-time phase separation process follows a crossover scaling form regardless of the particle shapes and dividing surface designs.

Rich lateral ordering behavior of JNs at the polymer blend interface has practical implications for the precise positioning of nanoparticles to fabricate nanostructured functional materials.

II. Application—3. LCs or its related complex systems

- The phase behavior, structure, and dynamics of rodlike mesogens with various flexibility
- The anchoring transitions driven by rod–coil amphiphiles at aqueous–liquid crystal
- the Phase Behavior of T−Shaped Ternary Amphiphiles Possessing Rodlike Mesogens

II. Application—3 rodlike mesogens with flexibility

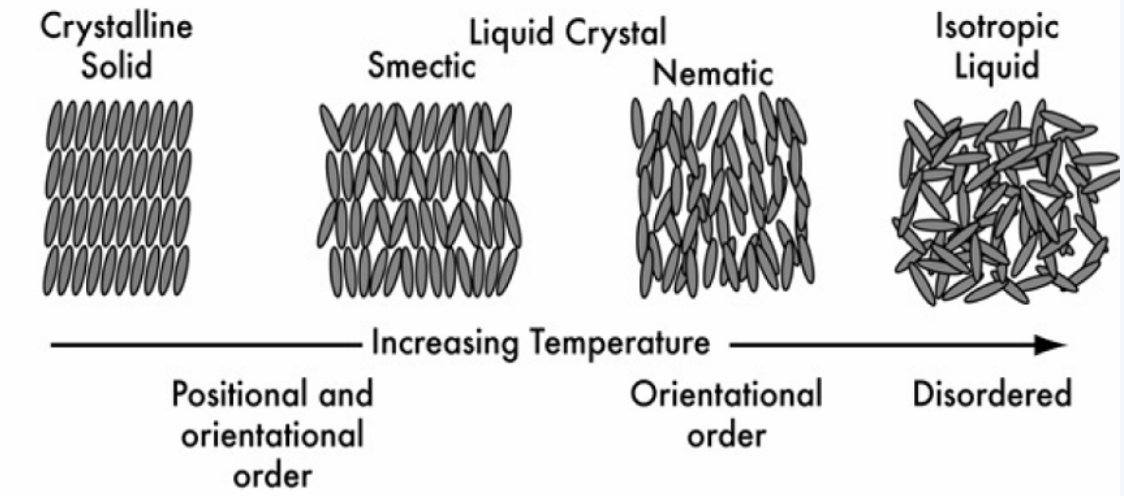

generic single site models :

- hard particle models : ellipsoids and sphero-cylinders with hard core repulsions

------computational simplicity, vailid for entropically driven lyotropic LC behavior but not for the thermotropic LCs

- soft particle models : Gay – Berne GB potential model

------soft ellipsoids with well-defined anisotropic attractive and repulsive interactions, a more realistic model

most LC molecules, LC polymer, exhibit some degree of flexibility have large effect on the stability of particular LC phase!!

➢effect of molecular flexibility on the LC phase behavior

Why DPD not MD:

- Mesophase formation in thermotropic LCs usually occurs in the mesoscopic length- and time-scales

DPD model for mesogen

1. rigid mesogen model

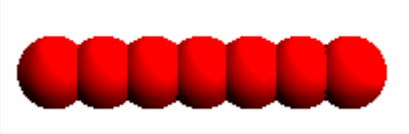

（Rod7、Rod6、Rod5）

+ **Rattle constraining algorithm**
(to keep the beads aligned and equidistant)

2. semirigid mesogen model: semirigid bead-spring model

+ bending potential

J. Chem. Phys. 113, 144911 (2010).

● Phase behavior of the rigid mesogen R_7

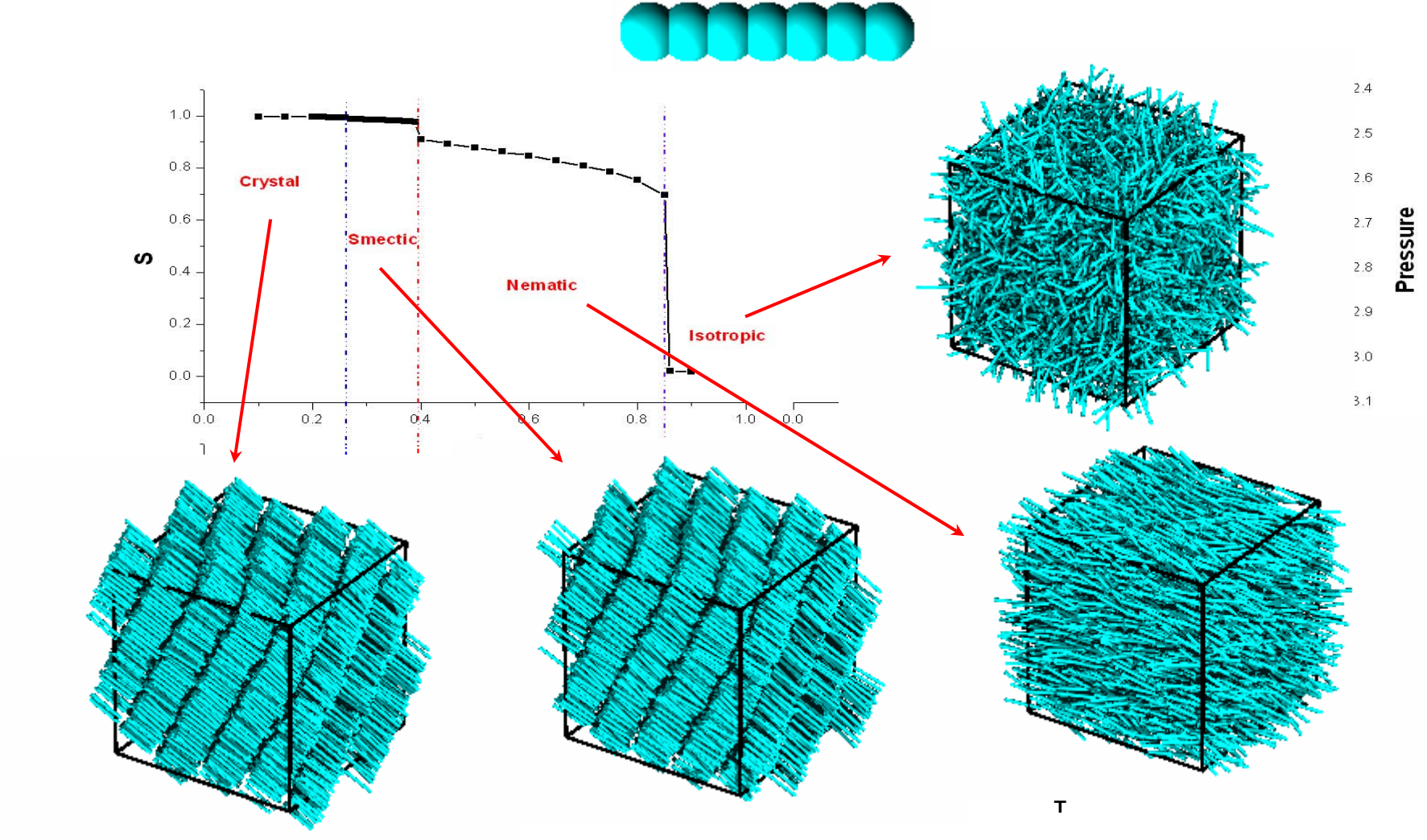

●The diffusion properties of R_7 in various LC phase

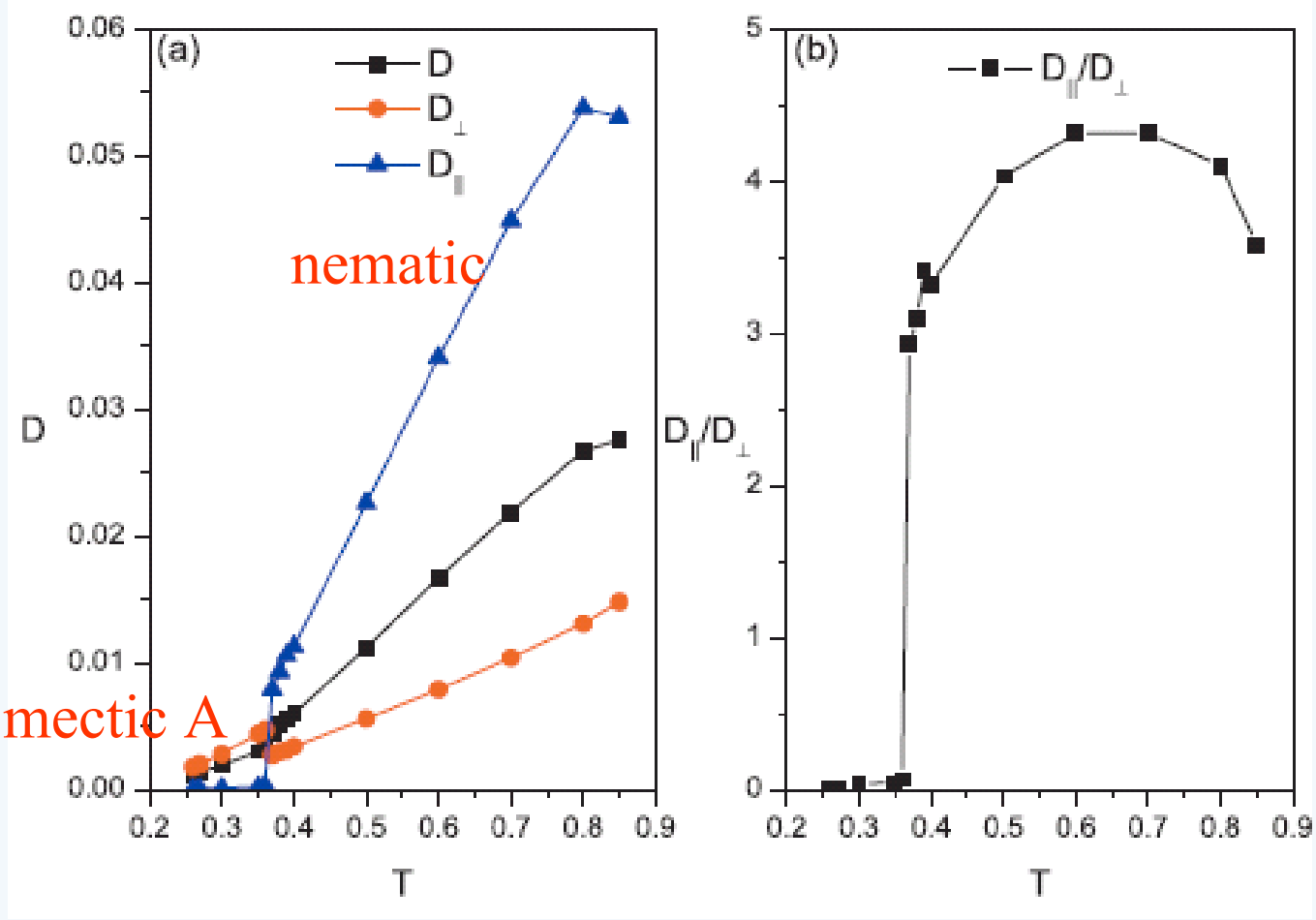

●The effect of rod length on the phase behavior

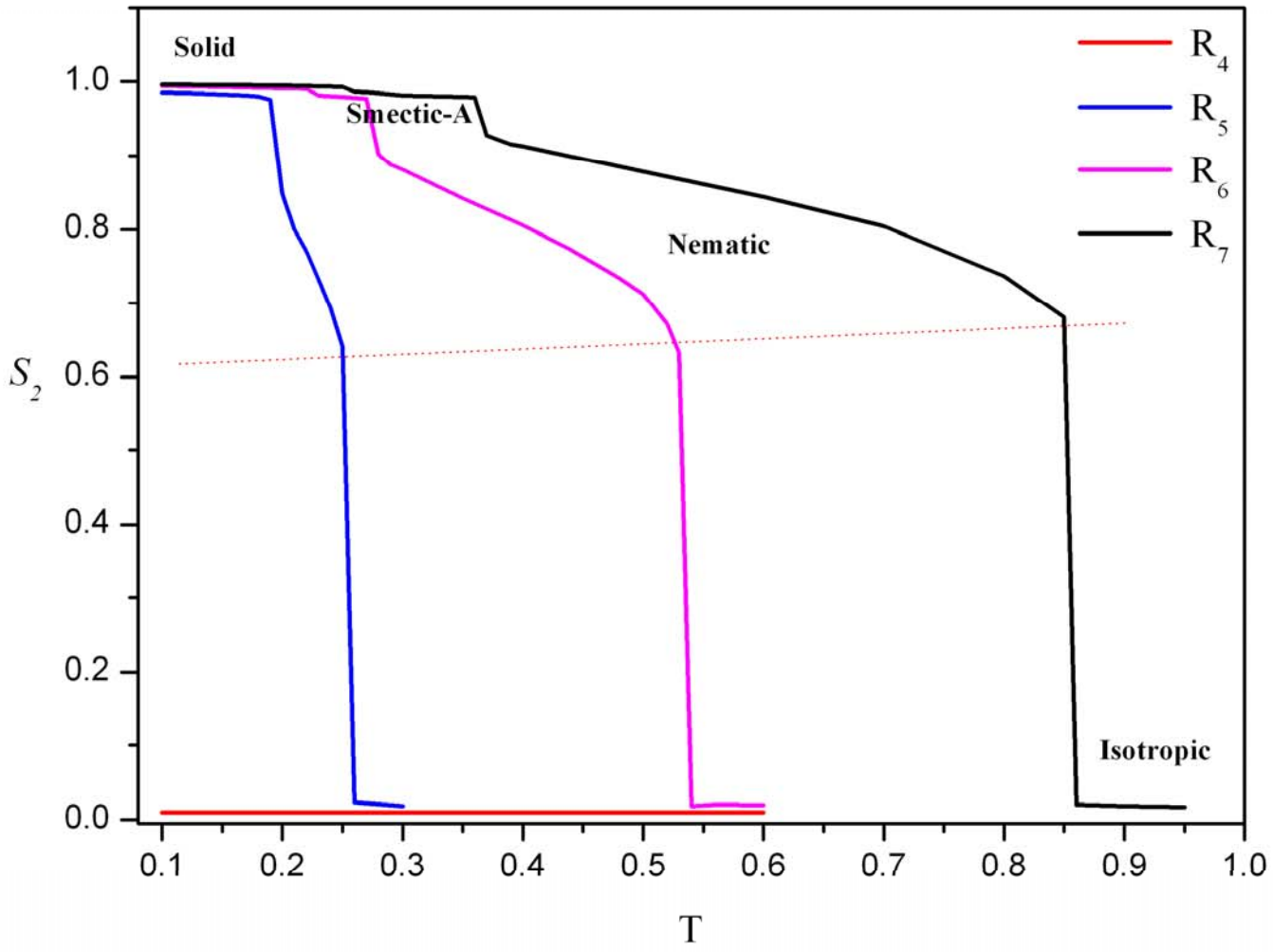

- The effect of molecular flexibility, k_Φ on the phase behavior

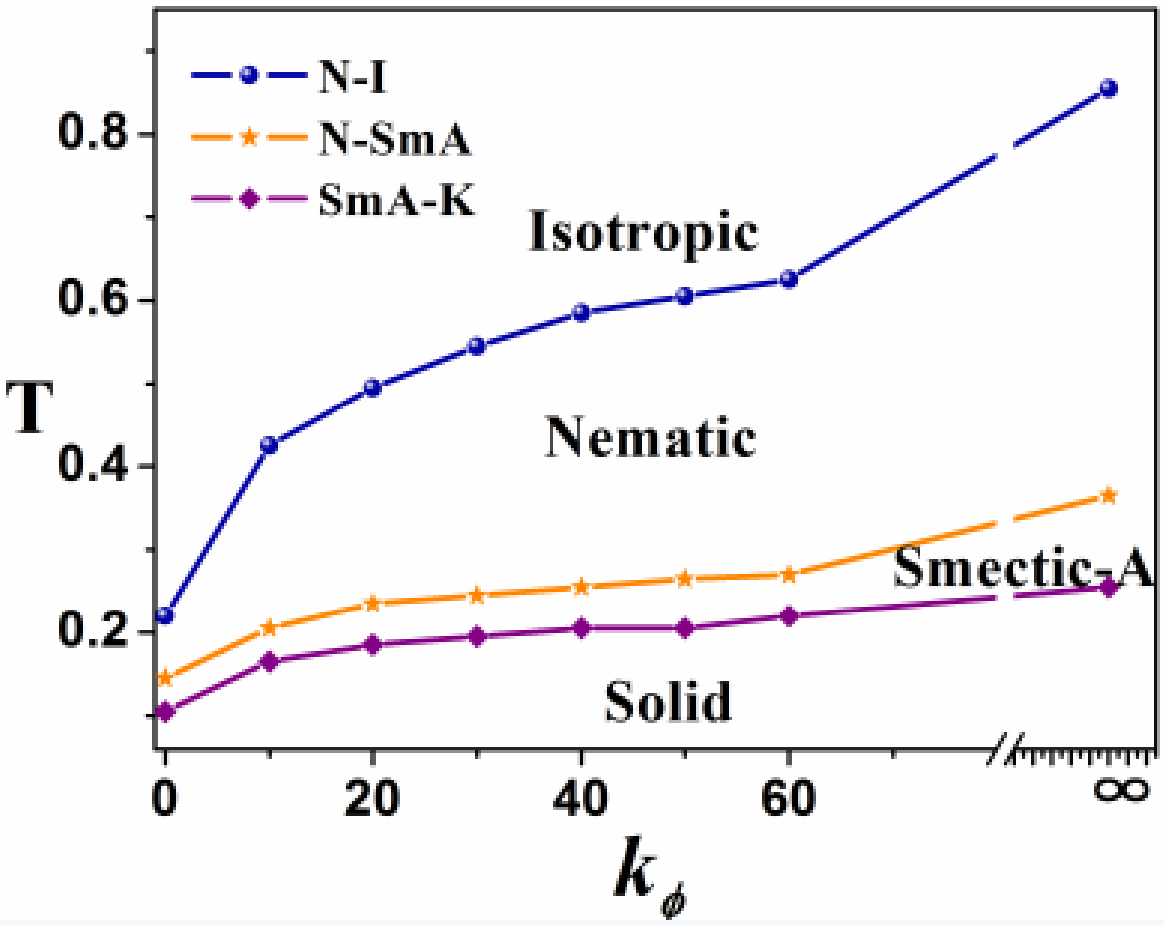

- Both the rigid model and the semirigid model capture the essential molecular features necessary for the formation of LC phases.
- The static and dynamic properties of LC phases have been efficiently reproduced.

Our extensive DPD simulations on these two models provide an important insight into the effect of molecular flexibility on thermodynamical, dynamical, and structural properties of the LC phases.

It is clear that dissipative particle dynamics is an extremely efficient mesoscale technique for numerical simulation of LC phases.

➢II. Application—3 rod–coil amphiphiles at aqueous–liquid crystal

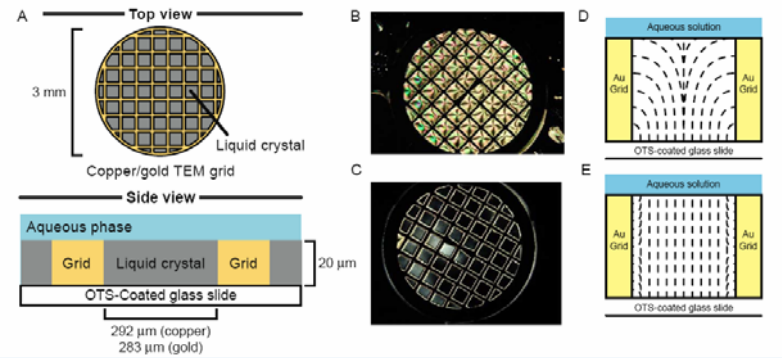

biological and medical sensor

anchoring transition of LCs at aqueous–LC interfaces provides a powerful tool for probing and amplifying the molecular events at the interfaces into visual optical imaging.

Nature **2007**, 6, 929-938

●anchoring transitions in the presence of amphiphile monolayer at the aqueous/LC interface

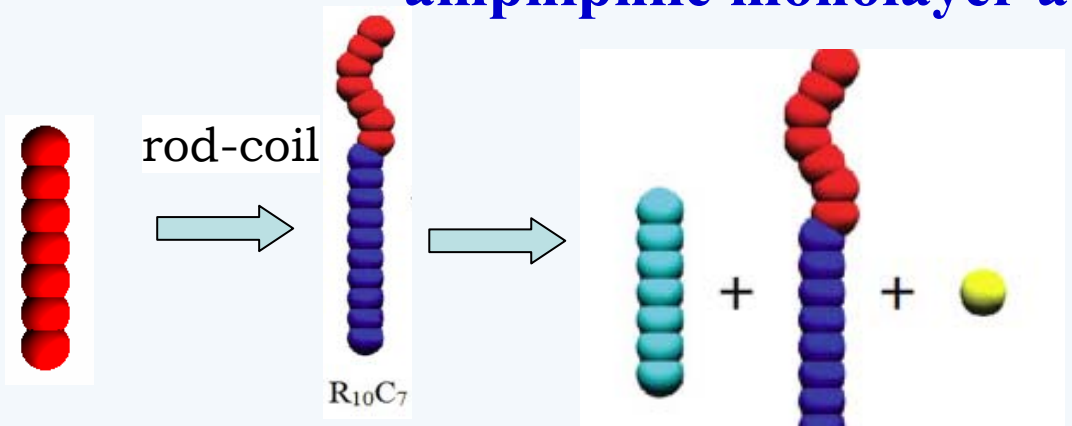

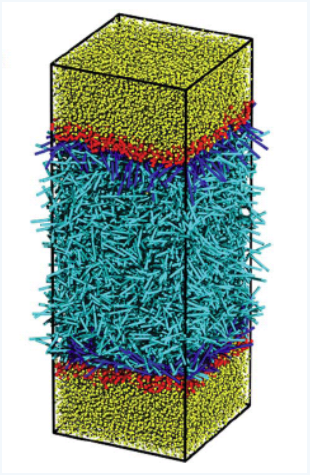

Mesogen M_7 + rod-coil amphiphile $R_{10}C_7$ + water C_1

Soft Matter, 8，5168-5174(2012)

➢II. Application—3 rod–coil amphiphiles at aqueous–liquid crystal

Anchoring transiotn with rod-coil content

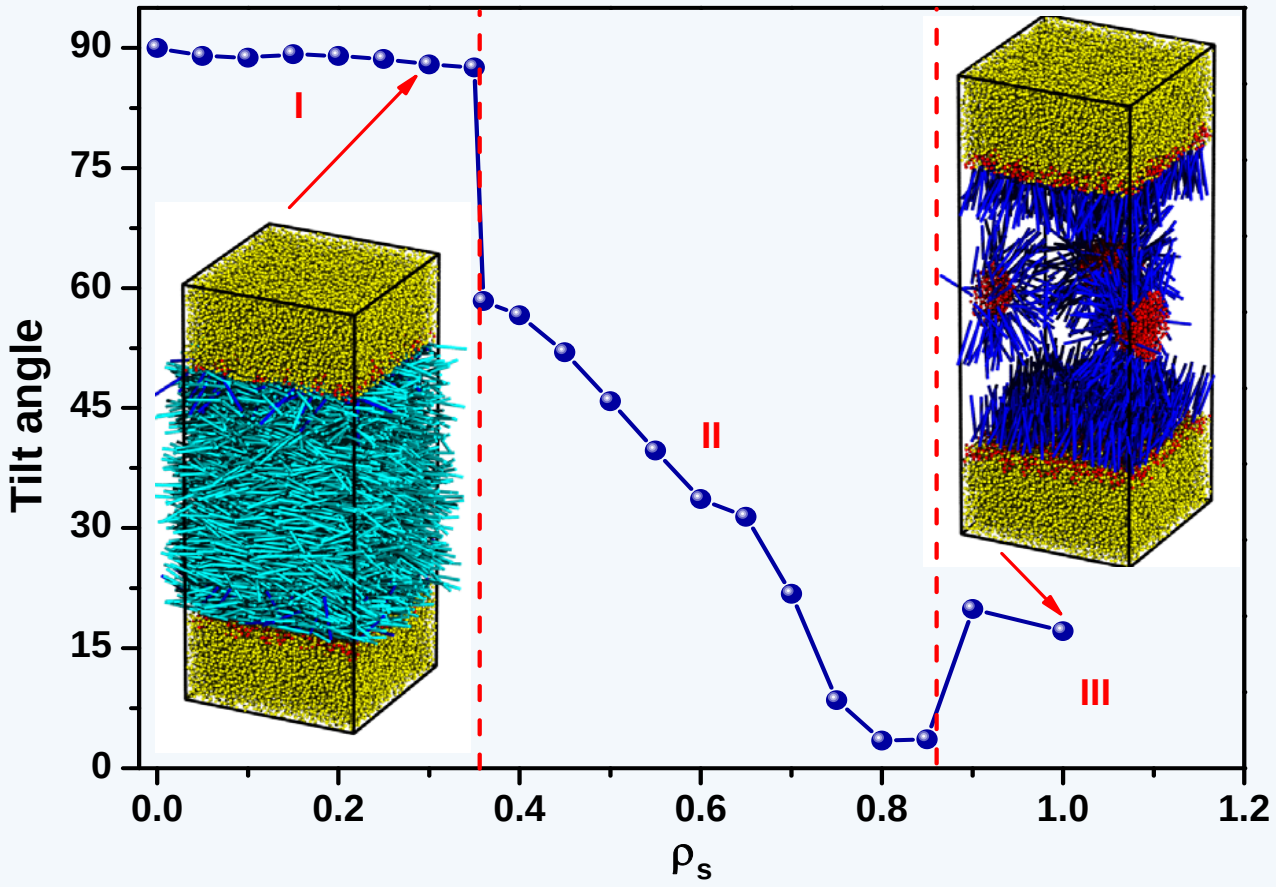

●Influence of the repulsion interaction parameter between the mesogens and the rod blocks of amphiphiles (aMR) on the anchoring behavior of liquid crystals

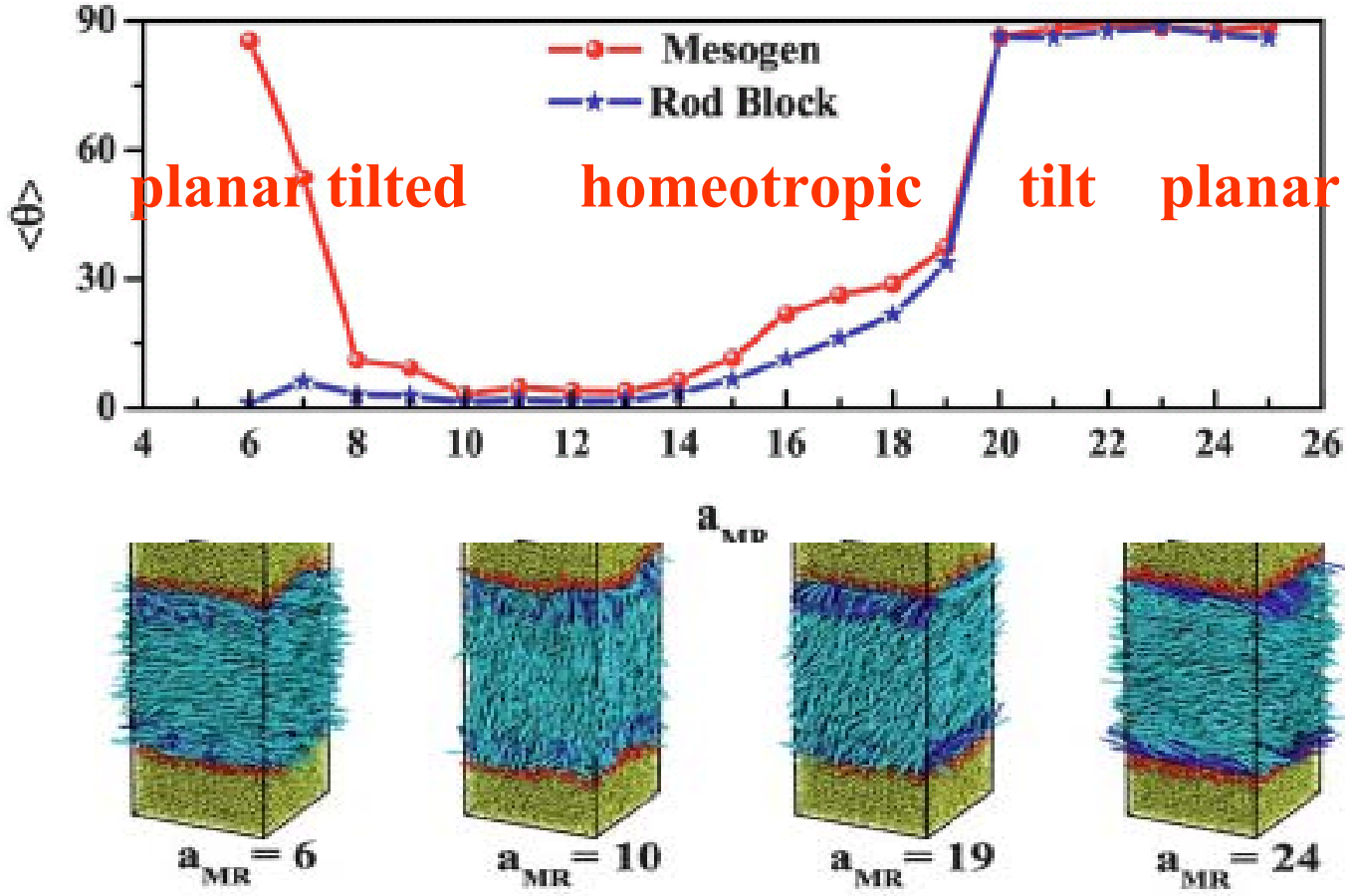

tuning aMR, which is essentially equivalent to changing the chemical constitution of the amphiphiles or the mesogens, enriches the possibility of tailoring the anchoring behavior at aqueous–LC interfaces.

➢II. Application—3 T−Shaped Ternary Amphiphiles Possessing Rodlike Mesogens

To fabricate the complex and highly ordered nanoscale or mesoscale structures, the practical strategy is to build molecules with the appropriate building blocks--**"bottom up" design**

T-shaped ternary liquid crystals (TLCs)

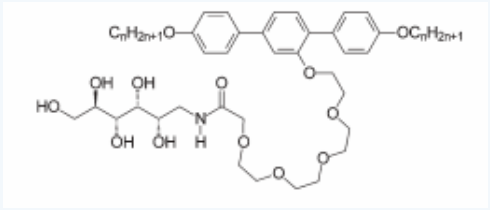

bolaamphiphile

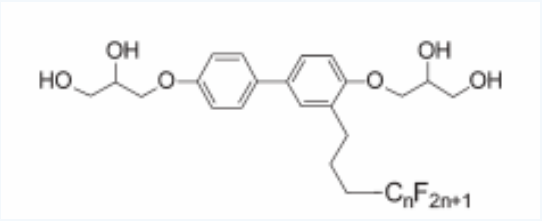

Facial amphiphile

Our interest

to understand how controlling the sizes of both terminal and lateral substituents affects the complex interplay of the entropic and enthalpic incompatibility of the system and in turn tunes the morphology formation of complex phases

Semirigid mesogen

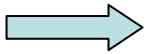

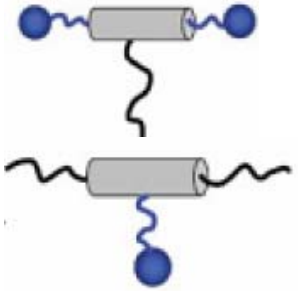

T−Shaped Ternary Amphiphile model

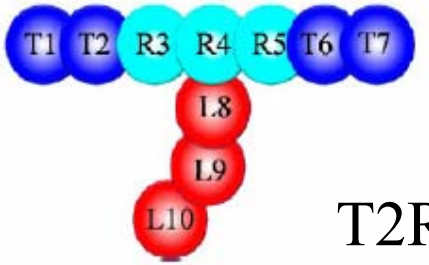

T2R3L3

- Phase Behaviorof T-Shaped Ternary Amphiphiles Possessing Rodlike Mesogens

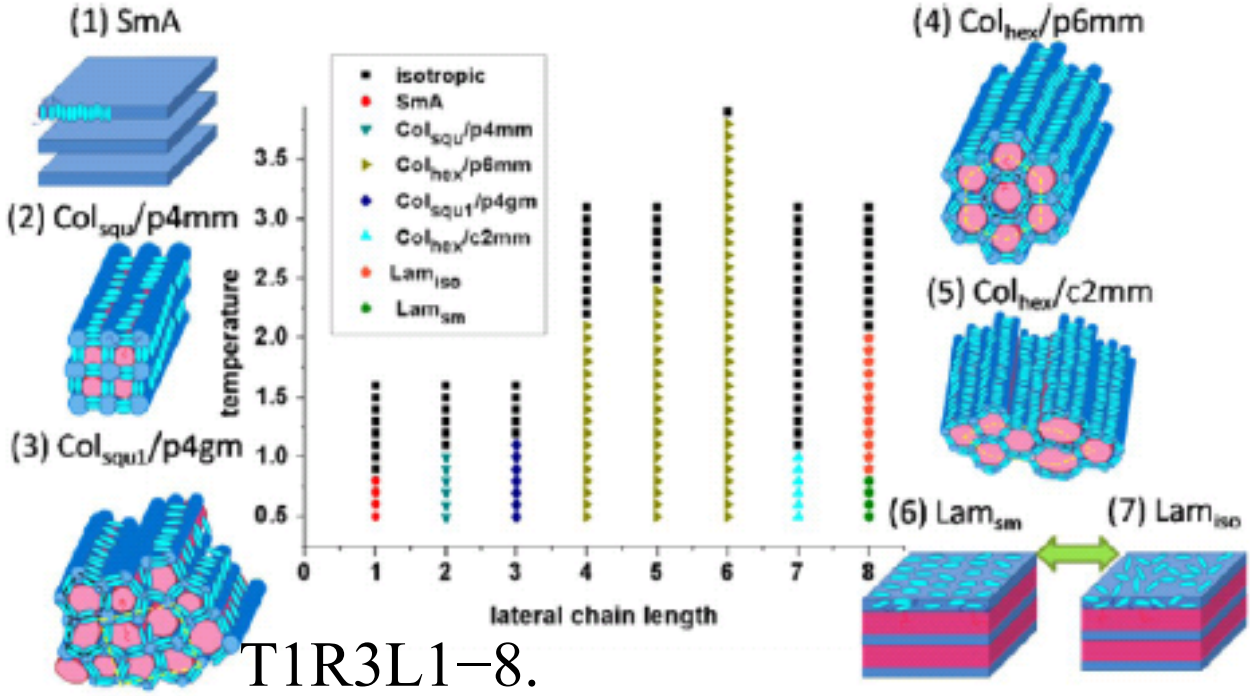

T1R3L1−8.

J. Phys. Chem. B, 117 , 9106 (**2013**)

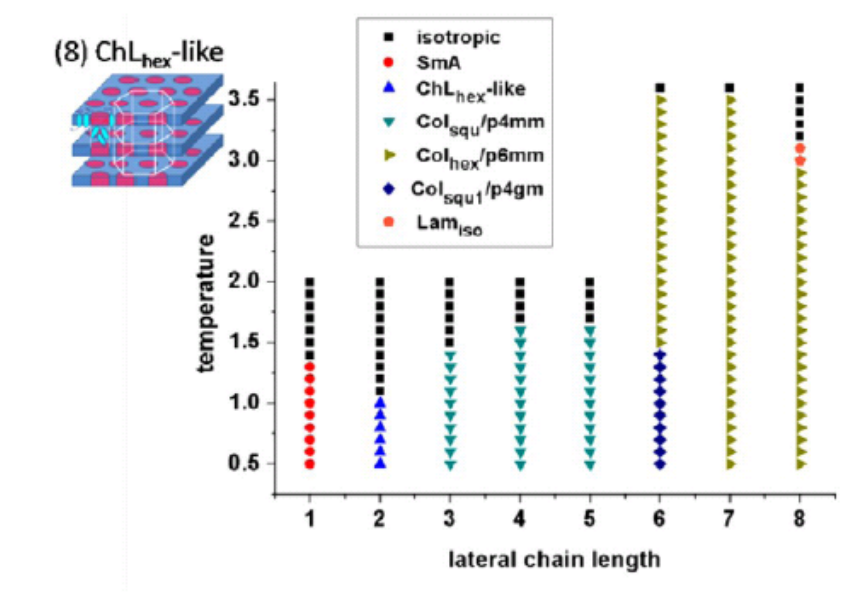

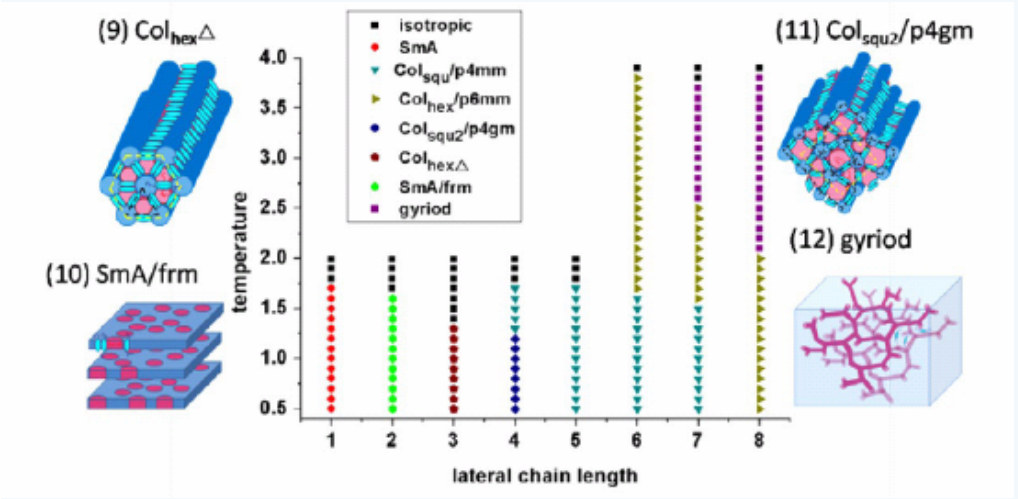

T2R3L1−8.

T3R3L1−8.

The volume fraction of lateral chains in TLCs is an important variable to influence the liquid crystalline behavior

$$f_L = \frac{(d_L^{prob})^3 \times N_L}{(d_R^{prob})^3 \times N_R + (d_T^{prob})^3 \times N_T + (d_L^{prob})^3 \times N_L}$$

J. Phys. Chem. B, 117 , 9106 (**2013**)

the universal phase diagram
as a function of effective volume fraction of lateral chains

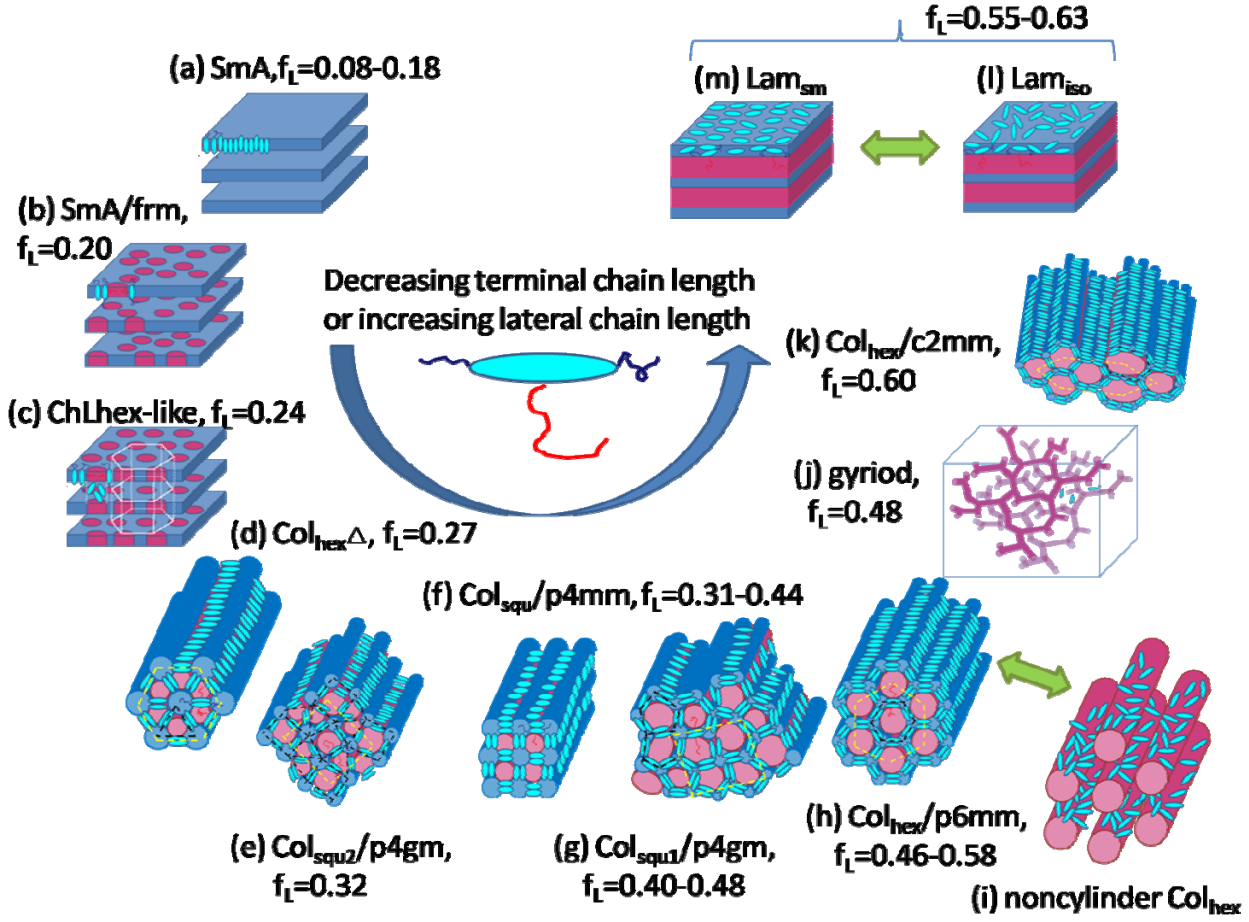

- quantitatively compared with the experimental results
- a unique view to understand the universal phase behavior in real TLCs systems

II. Application—4. lipid

- Phase Behavior of Lipid Bilayers
- Protein-Mediated Vesicle Fusion

➢II. Application—4 lipid

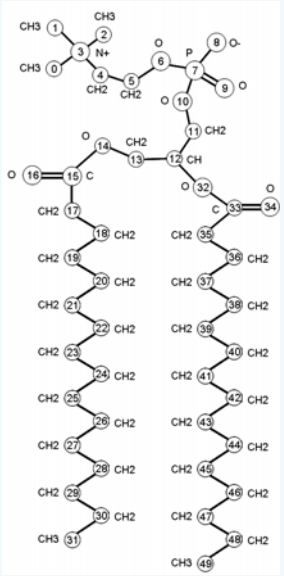

DPPC

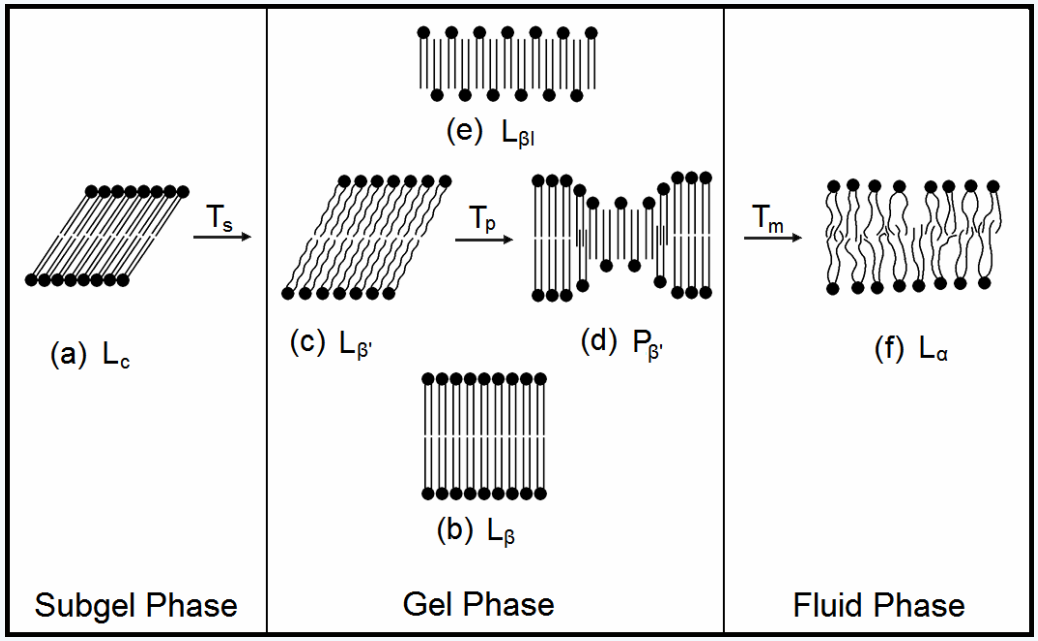

Our interest

A detailed understanding of the gel phase and their relevant transitions is therefore of great biological interest. On the other side, the lipid molecules are restricted in the membrane plane, which makes the lipid bilayer a perfect model for studying two-dimensional phase transition.

➢Phase Behavior of Lipid Bilayers

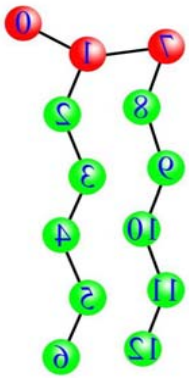

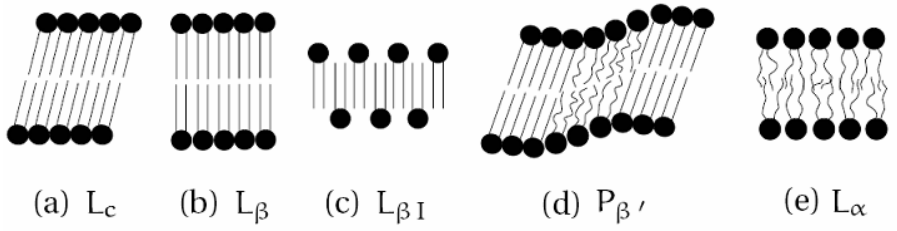

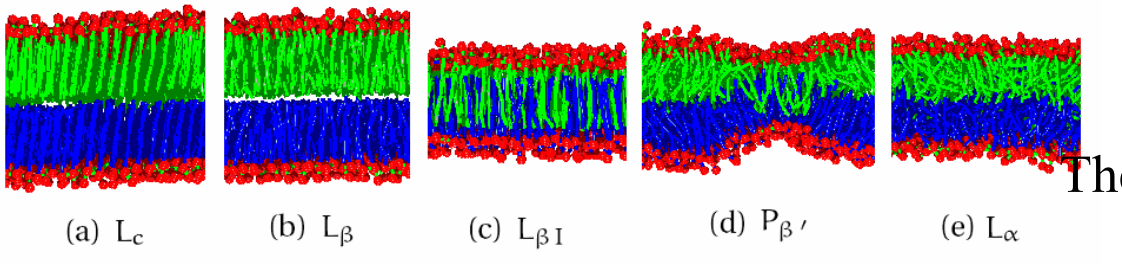

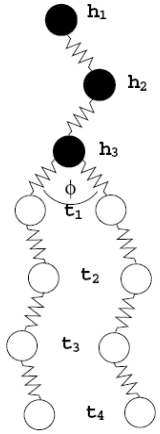

The CG model by Smit.

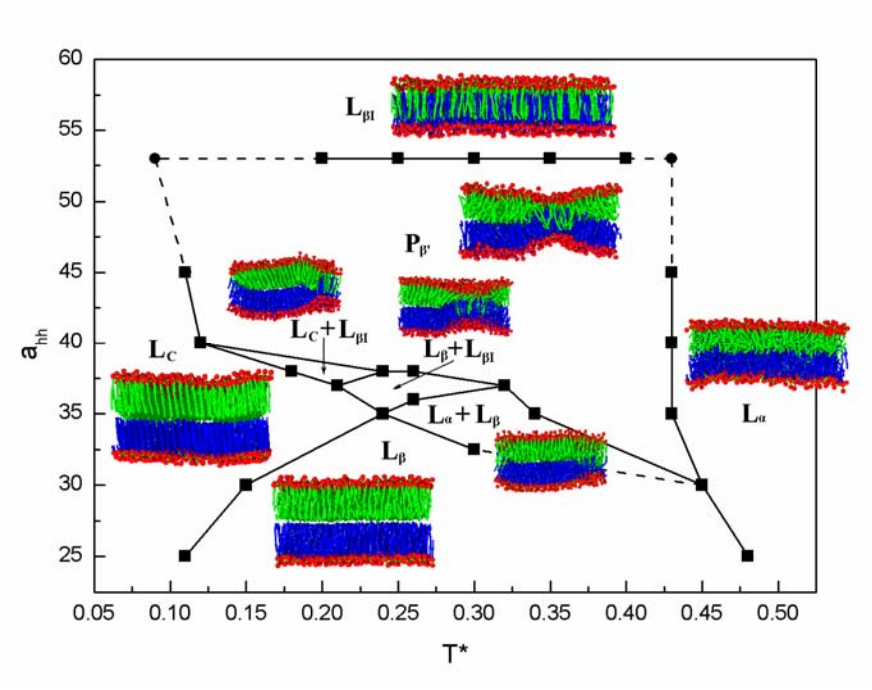

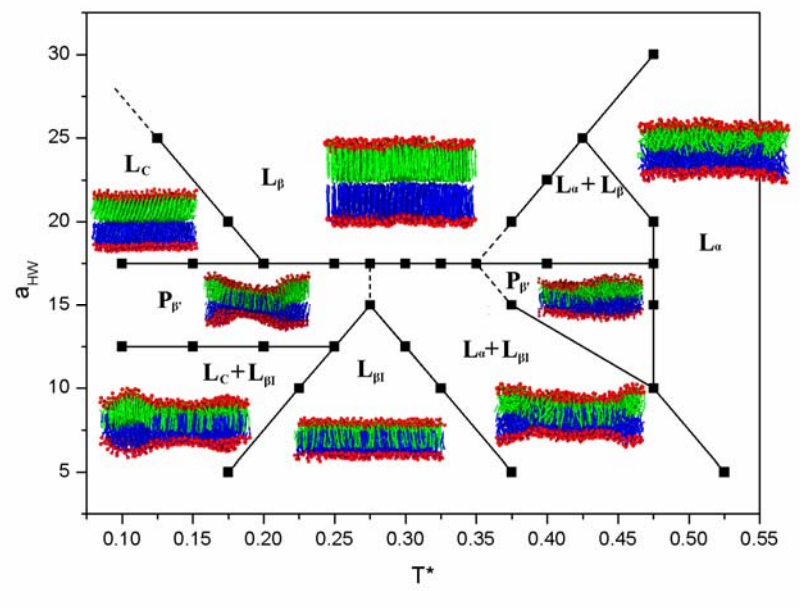

Front. Chem. China 2010, 5(3): 288–298

➢Protein-Mediated Vesicle Fusion

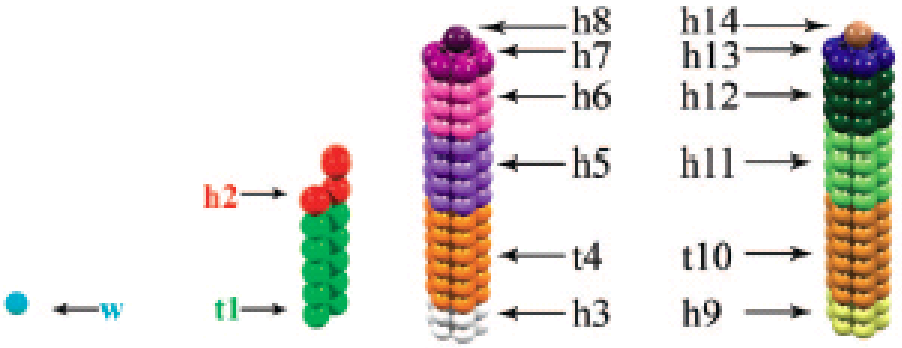

(a) water (b) lipid (c) t-protein (d) v-protein

a simple model system to mimic the complicated protein-mediated vesicle fusion involving extensive and cooperative molecular rearrangement!!!

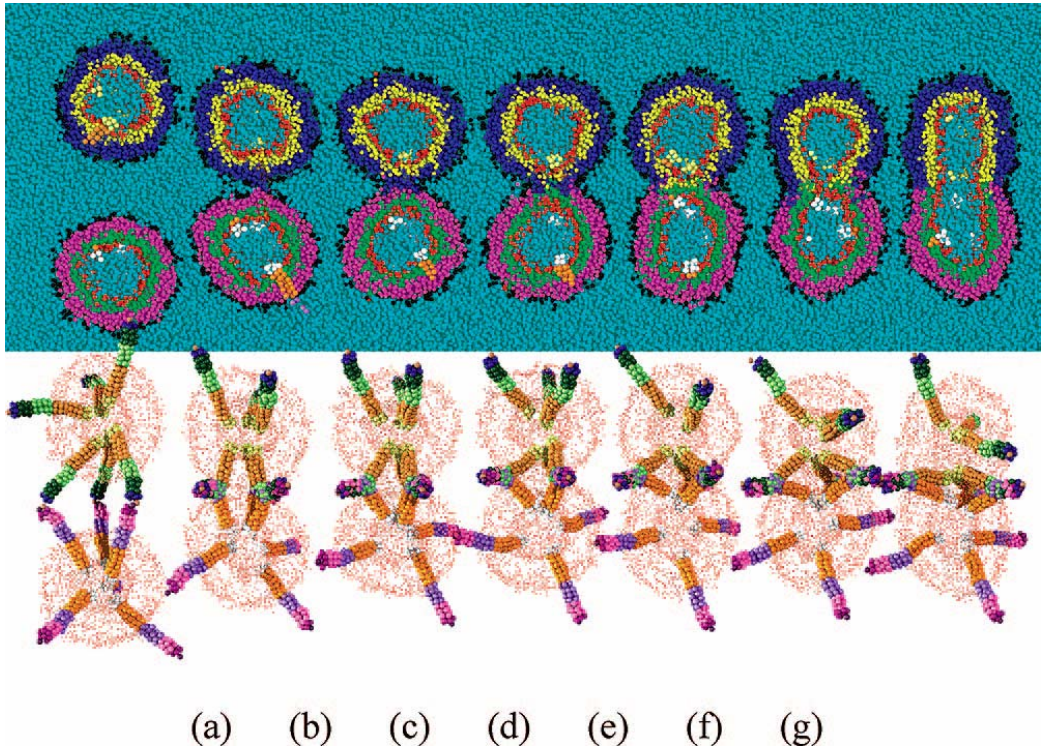

Pathway I of protein-mediated vesicle fusion (scaffold model):

(a) starting state; (b) outer leaflets contact; (c) stalk; (d) inner leaflets contact; (e) hemifusion diaphragm; (f) fusion pore appears; (g) full fusion

J. Phys. Chem. B, 113, 589 (2009)

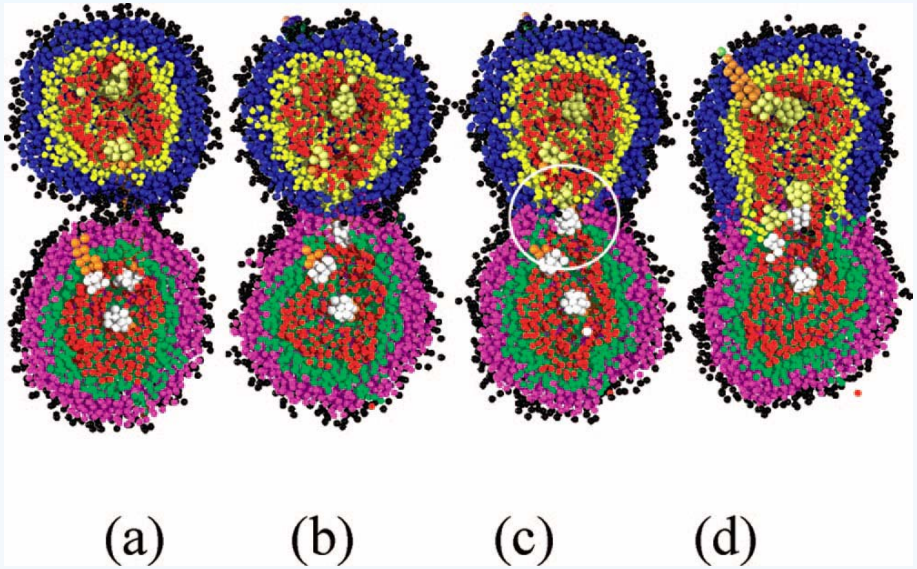

Pathway II of protein-mediated vesicle fusion (protein-pore model). The protein-lined pore (encircled) originates directly from the radially expanding stalk, which allows lipid and water to penetrate into it. Then, the pore expands to accomplish vesicle fusion: (a) outer leaflets contact; (b) stalk; (c) protein-lined fusion pore appears; (d) full fusion.

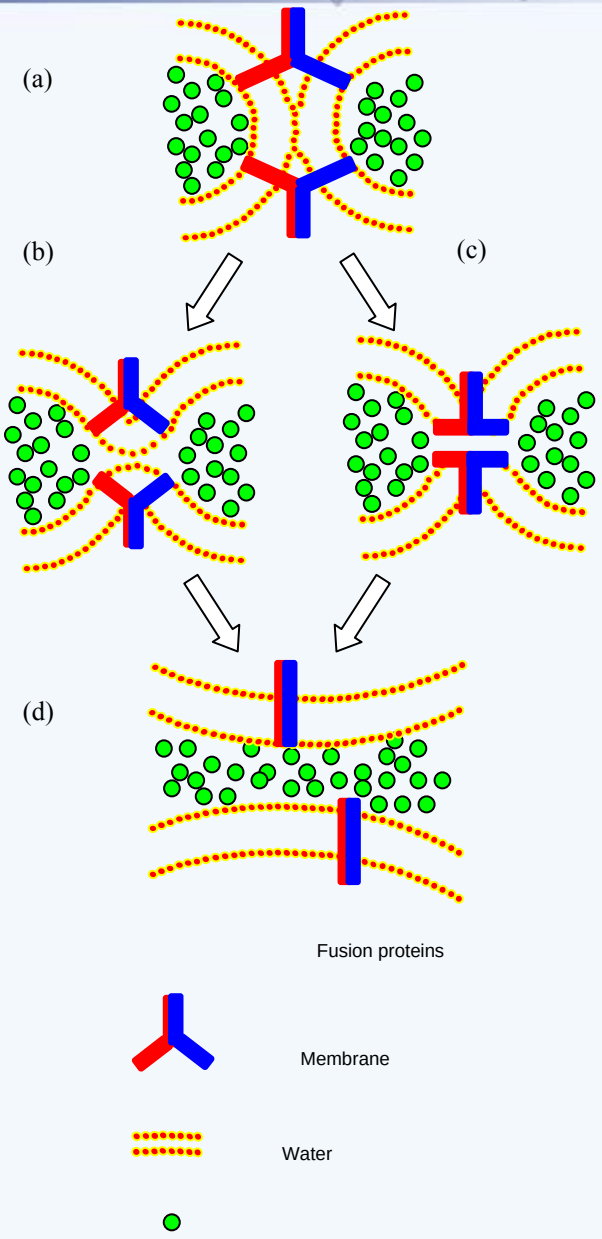

III. Application of DPD thermostat in--- 1. (NE)MD with LJ potential (spherical model system)

—2. (NE)MD with GB potential (non-spherical model system)

Application of DPD thermostat in 1. (NE)MD with LJ potential

Thermostats: to mimic the experiment conditions, to study the temperature dependent processes, to remove the excess heat generated by external fields

DPD thermostat and soft conservation potential are completely independent!!

DPD thermostat

- **stochastic, a large simulation time step**
- **conserve both the global and local momentums so that hydrodynamic behavior**
- **Galilean invariance, the solution of the thermal motion from the total motion is not necessary in NEMD**

well-known thermostats : Gaussian, Nosé-Hoover, Langevin

great applications in studying the dynamics of various complex fluids under non-equilibrium conditions!!!!

Stochastic thermostats in NEMD

Langevin Eq

$$m_i \ddot{\vec{r}}_i = \vec{F}_i - \zeta \dot{\vec{r}}_i + \vec{F}_i^{rand}$$

Langevin PBT

$$m_i \ddot{\vec{r}}_i = \vec{F}_i - \zeta (\dot{\vec{r}}_i - \gamma r_{iz} \vec{i}) + \vec{F}_i^{rand}$$

Langevin YZ

$$m_i \ddot{r}_{iy} = F_{iy} - \zeta \dot{r}_{iy} + F_{iy}^{rand}$$

$$m_i \ddot{r}_{iz} = F_{iz} - \zeta \dot{r}_{iz} + F_{iz}^{rand}$$

DPD

$$m_i \ddot{\vec{r}}_i = \vec{F}_i + \vec{F}_i^{D} + \vec{F}_i^{R}$$

$$\vec{F}_i^{D} = \sum_{i \neq j} \vec{F}_{ij}^{D}, \vec{F}_{ij}^{D} = -\zeta w^{D}(r_{ij})(\hat{\vec{r}}_{ij} \bullet \dot{\vec{r}}_i)\hat{\vec{r}}_{ij}$$

$$\vec{F}_i^{R} = \sum_{i \neq j} \vec{F}_{ij}^{R}, \vec{F}_{ij}^{R} = \sigma w^{R}(r_{ij}) \theta_{ij} \hat{\vec{r}}_{ij}$$

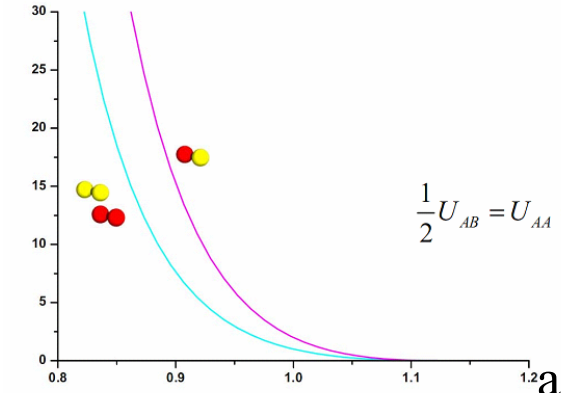

$M_A = 1.0$

$M_B = 10.0$

$$\frac{1}{2}U_{AB} = U_{AA} = U_{BB} = 4\times\left[\left(\frac{1}{r}\right)^{-12} - \left(\frac{1}{r}\right)^{-6} + \frac{1}{4}\right]$$

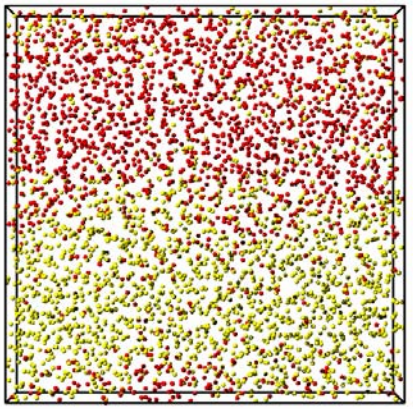

a binary mixture of LJ particles separate under shear flow

the streaming velocity profile of system should not be linear!!!

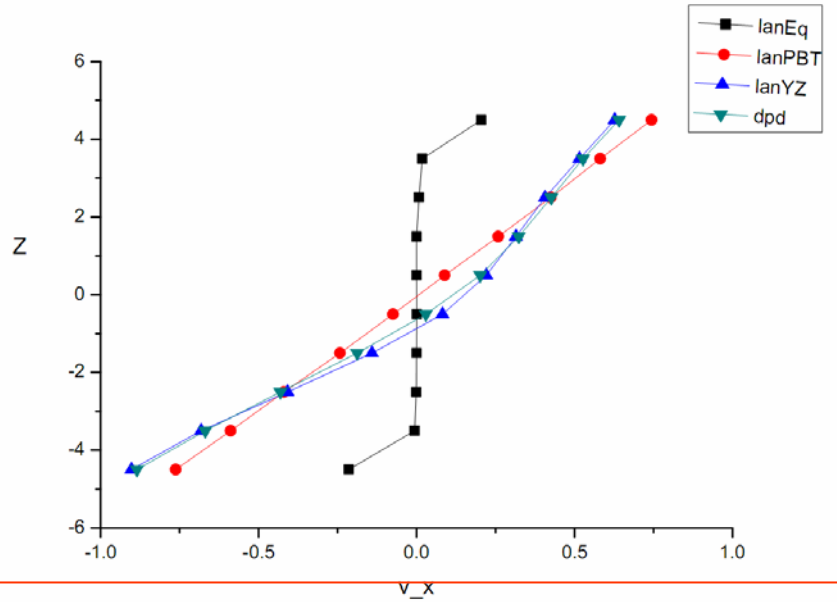

DPD thermostat is an ideal thermostat for NEMD simulations since it avoids profile biasing of NEMD simulation in a very natural and simple way, and thus suitable to study nonlinear phenomena in the nonequilibrium systems.

●DPD thermostat in NEMD of diblock copolymer melts

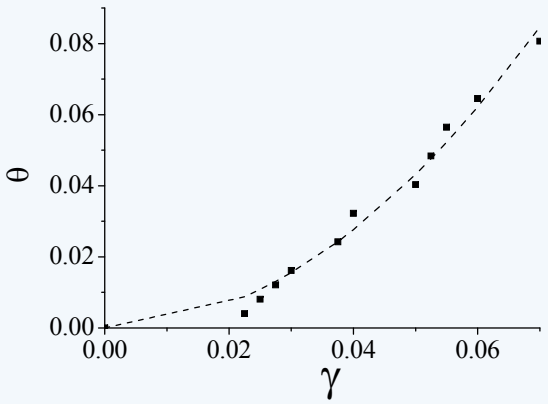

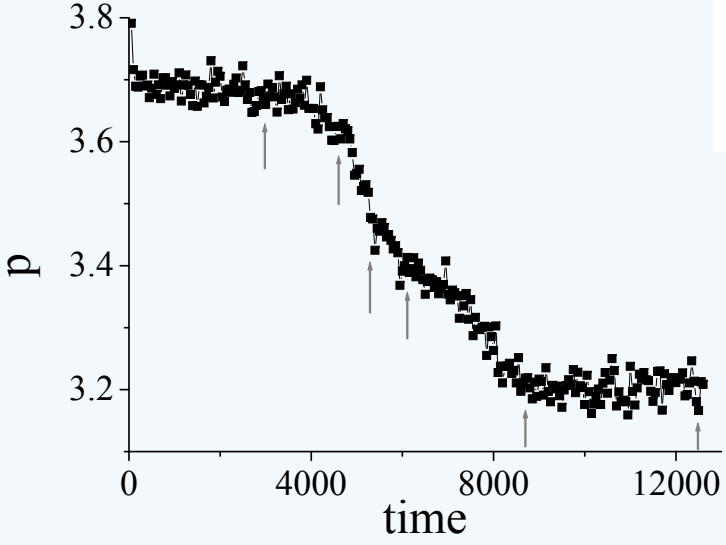

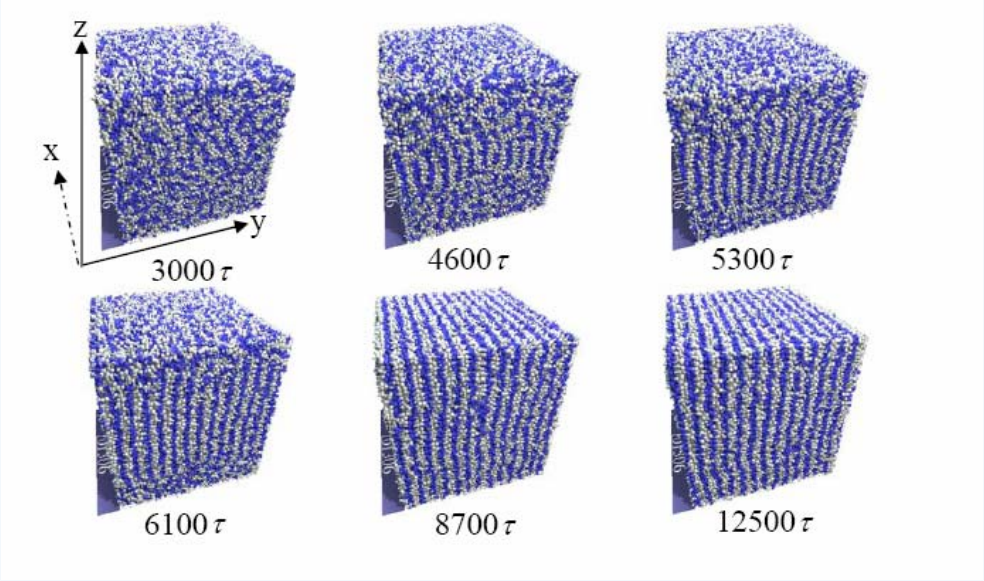

HX GUO， *J. Chem. Phys*, 127(5),054902-1-10 (**2007**)； 125(21), 214902-1-9 (**2006**)
J. Chem. Phys, 124(5), 054902-1-11 (**2006**)

***trans*-1,4-PB**

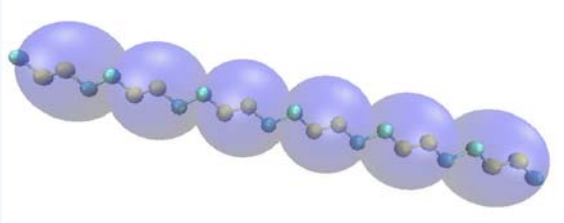

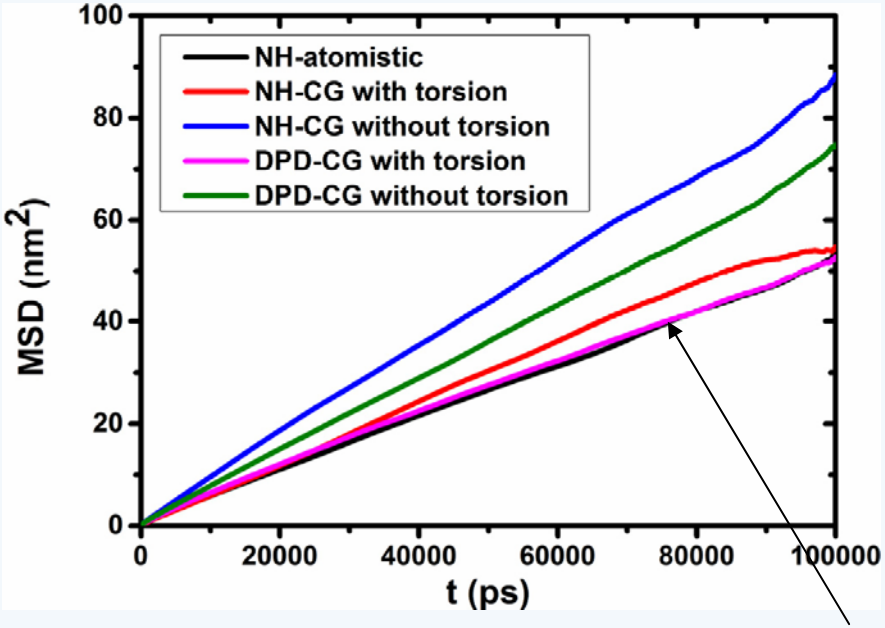

a standard DPD thermostat to remedy the removed degrees of freedom and reduced friction during CG and CG model can completely mimic the dynamics of the atomistic model

Polymer, 69,:25 (2015).

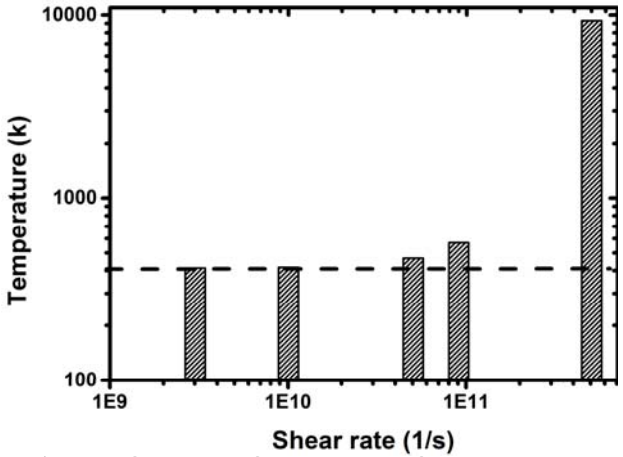

target temperature 413K

with the dissipation force factor of ɣ =0.056*10-13 Ns/m

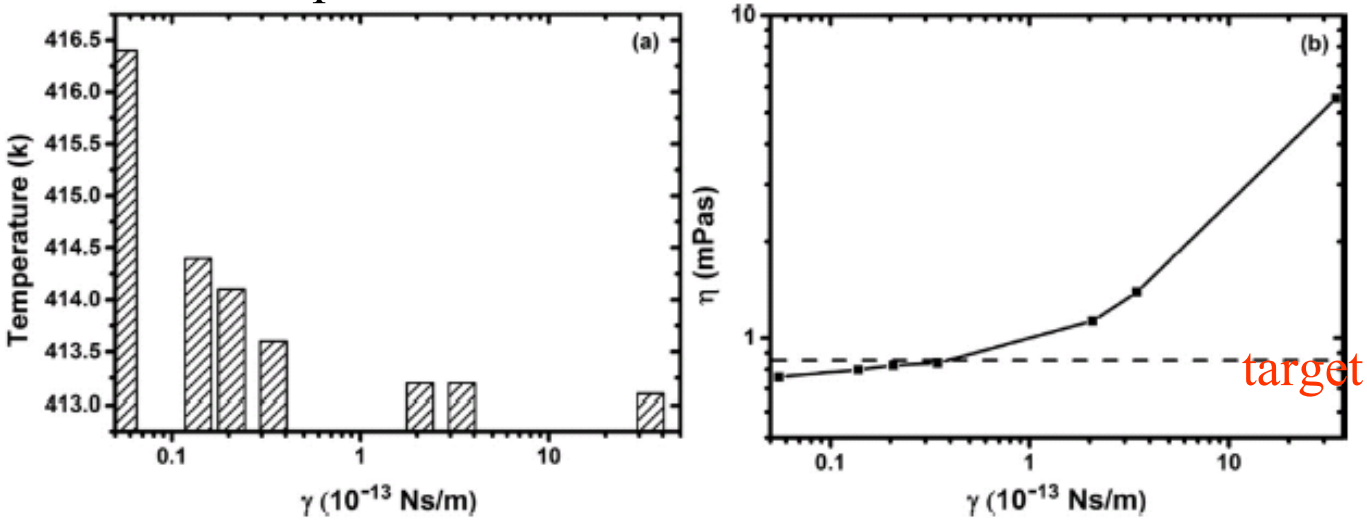

target shear viscosity

as a function of ɣ at a typical moderate shear rate of 1*1010 1/s (Wi =31.8)

standard DPD thermostat approach is applicable to the steady shear flow simulation at low and moderate rates and the relevant dissipative factor derived by matching diffusion coefficients can only quantitatively reproduce the shear viscosity at low shear rates.

➢Application of DPD thermostat in--- 2. (NE)MD with GB potential (non-spherical model system)

- Translational DPD (T-DPD) Thermostat
- Rotational DPD (R-DPD) Thermostat

T=0.95	Δt=0.002	Δt=0.006		Δt=0.012	
TEM	NH	T-DPD	R-DPD	T-DPD	R-DPD
0.30	0.949±0.012	0.946±0.019	0.948±0.019	0.935±0.019	0.946±0.019
0.32 ρ	0.949±0.013	0.946±0.017	0.948±0.018	0.937±0.018	0.950±0.020
0.34	0.949±0.017	0.949±0.019	0.954±0.019	0.940±0.018	0.930±0.019
0.36	0.949±0.018	0.949±0.019	0.948±0.019	0.945±0.019	0.942±0.020

Sci China Chem, 2015, 58(4): 694–707

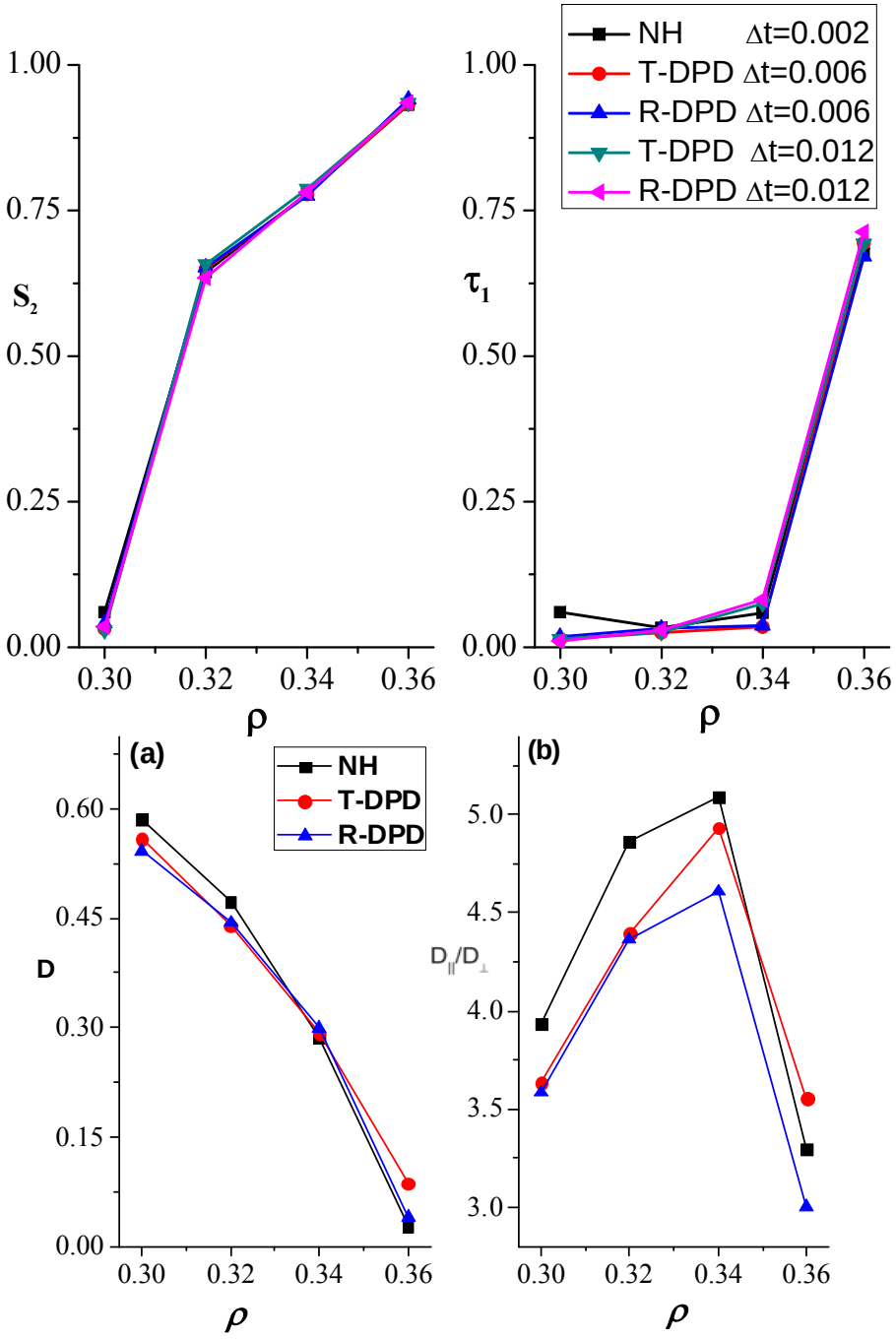

orientational order parameter *S*2

translational order parameter τ 1

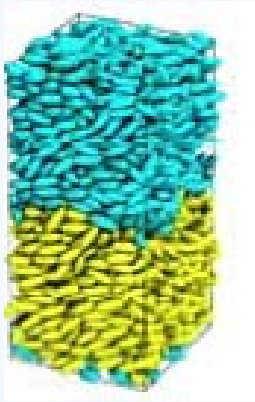

a binary mixture of LJ particles separate under shear flow

the mass ratio of particle B to A is set to 10

streaming velocity profile should not be linear!!!

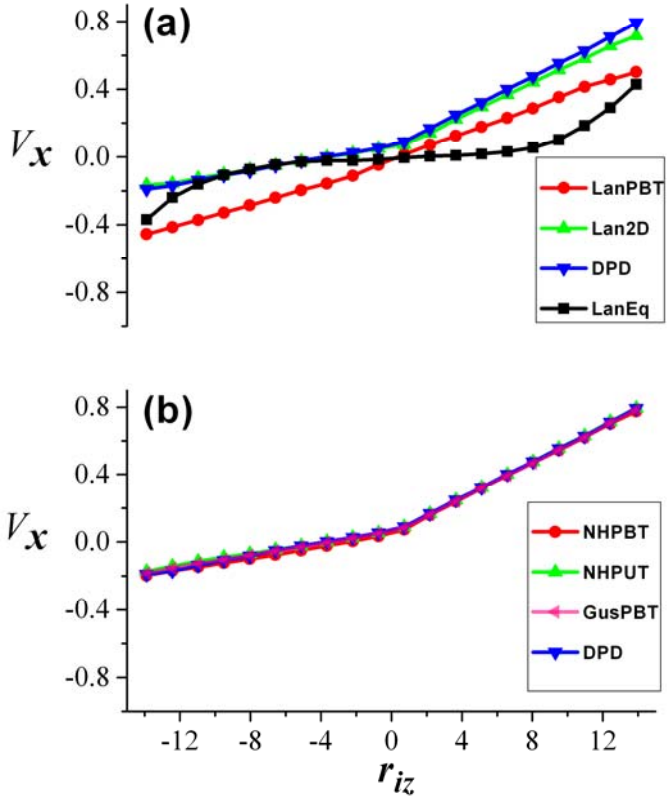

Lan2D or DPD thermostat,
the streaming velocity profile displays the expected broken line feature

GusPBT and NosPBT: we assumed the streaming velocity profile linear which conflicts with the above simulation results, these two thermostats are not reliable.
NosPUT and DPD thermostats works without linear profile hypothesis and can achieve the correct streaming velocity profile.

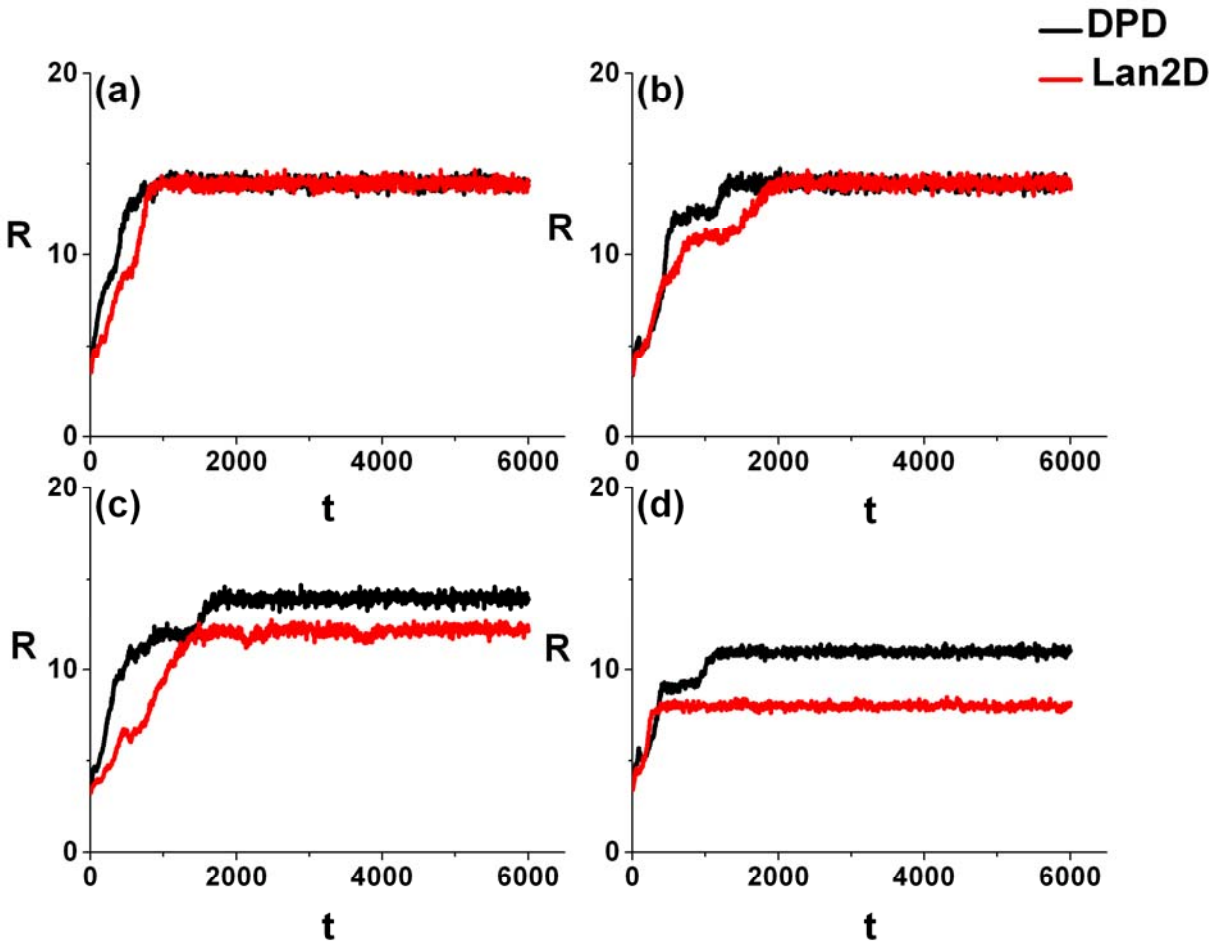

DPD thermostat conserves both global and local moments of system,
it wouldn't screen hydrodynamic interactions
promotes the phase separation.

➢Application of DPD thermostat in--- 2. (NE)MD with GB potential (non-spherical model system)

- translational T-DPD and rotational R-DPD thermostats : used in the GB system independently and both can achieve the thermostatting effects.

- a time step of $\Delta t = 0.012$ and a dissipative coefficient of $\zeta t = 0.01-0.1$

- avoids profile biasing of NEMD simulation

- unscreen hydrodynamic interactions

IV. Efficient and large-scale dissipative particle dynamics simulations on GPU

speeding up the computation of DPD to study large-scale systems at reasonable computational cost is one of the important subjects in computational chemistry and computational material science!!!

Keda Yang, Zhiqiang Bai, Jiaye Su,Hongxia Guo, Efficient and Large-Scale Dissipative Particle Dynamics Simulations on GPU, *SOFT MATER.*, **2014**, 12, 2: 185-196

IV. Efficient and large-scale dissipative particle dynamics simulations on GPU

✓a systematic framework for implementing DPD on GPU is still lacking

takes advantage of the superior computational performance of GPUs allows for highly efficient and large-scale DPD simulations

✓To develop highly efficient and large-scale GPU-based DPD,

the scheme for GPU implementation should also be designed and optimized according to the nature of DPD simulation technique, optimizing techniques specific for DPD should be included.

Rozen et al.have developed GPU-based DPD, suffer the low speed of the scattered data access in the linked lists

Implementation of DPD simulation on a GPU

(a) Set up the initial conditions for the simulation

(b) Perform the first stage of numerical integration during a single δt

(c) Update the neighbor list.

(d) Perform the second stage of each numerical integration step.

Firstly, the new non-bonded interactions between any pair of DPD particles are evaluated

Then the new bonded interactions such as harmonic bond forces and angle forces are calculate

Finally, the velocity of each particle is updated

(e) Loop over steps (b)-(d) until the simulated system reaches an equilibrium state or long enough to study nonequilibrium phenomena

Implementation of DPD simulation on a GPU

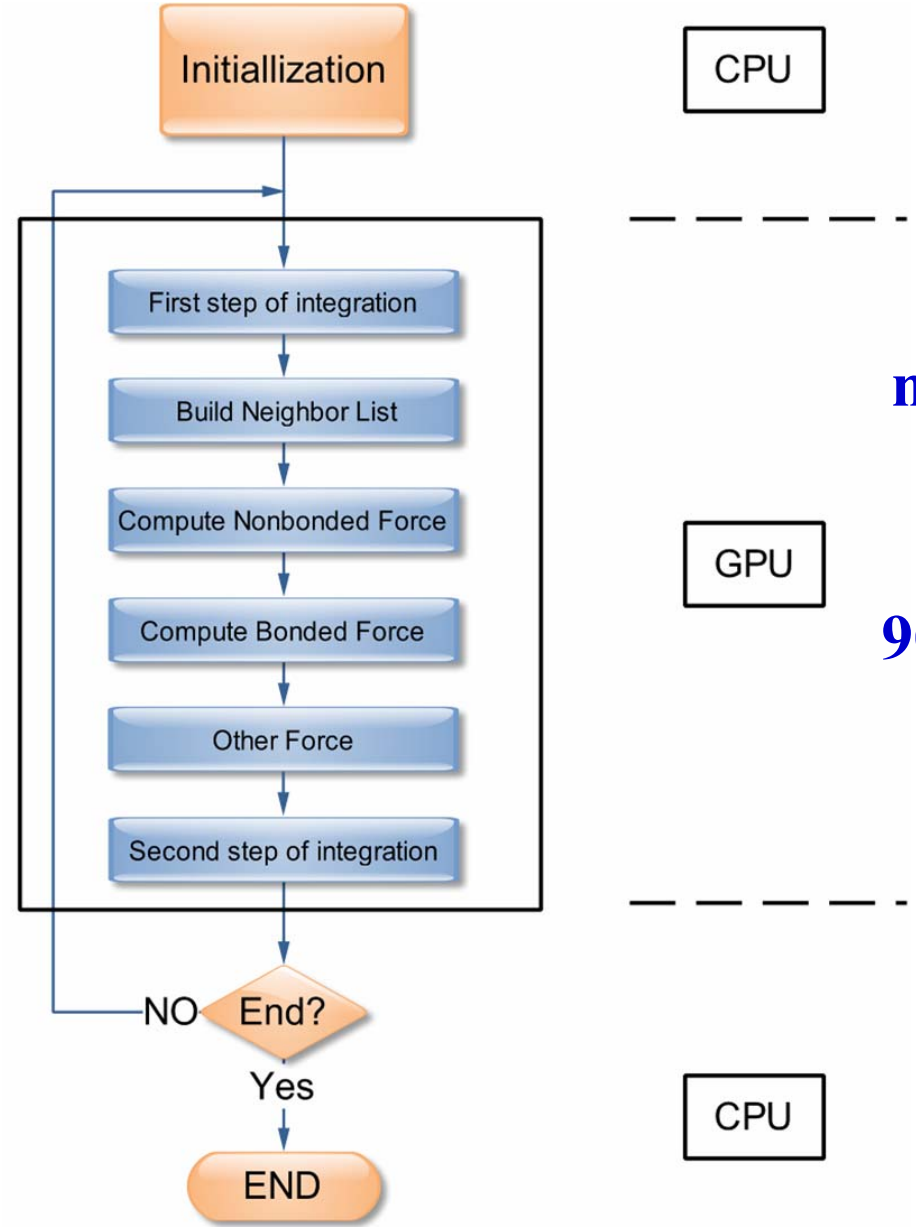

more computationally intensive and consume more than 90% of simulation time

some optimizations on *Neighbor list construction*

(i) the neighbor list is constructed without a surrounding shell and updated in each step.

(ii) a modified particle reordering technique is introduced to improve the device memory access efficiency for generating neighbor lis

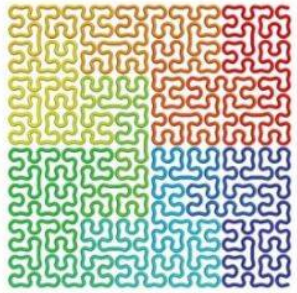

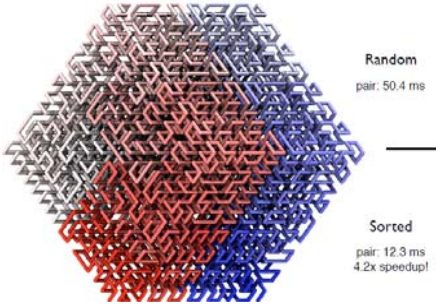

Storing the data as cell index
1.Effective
2.Easy to implementation

（iii）we loop over all particles directly during the neighbor list generatior without using shared memory and looping over cells first

Non-bonded force computation

the uniformly distributed random numbers generated by *sarua (novel hash-based PRNG*) are transformed into the normally distributed ones by the Box-Muller method.

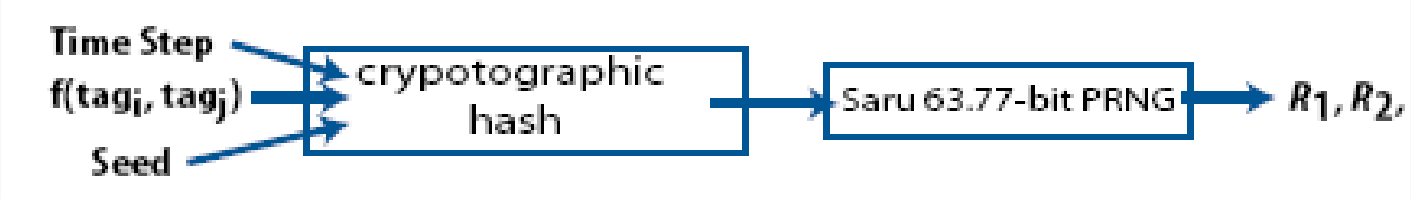

In this way, not only the same stochastic forces can be obtained for the *i*-*j* and *j*-*i* pairs, but also less GPU time is taken.

Algorithms for large-scale simulations

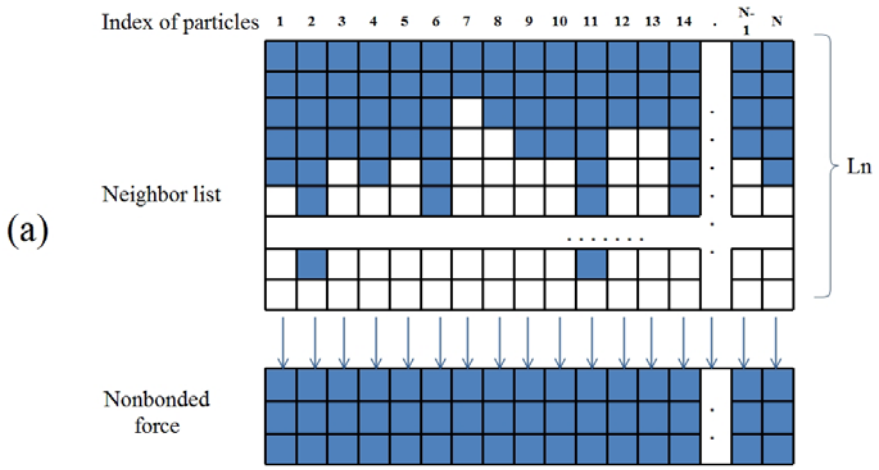

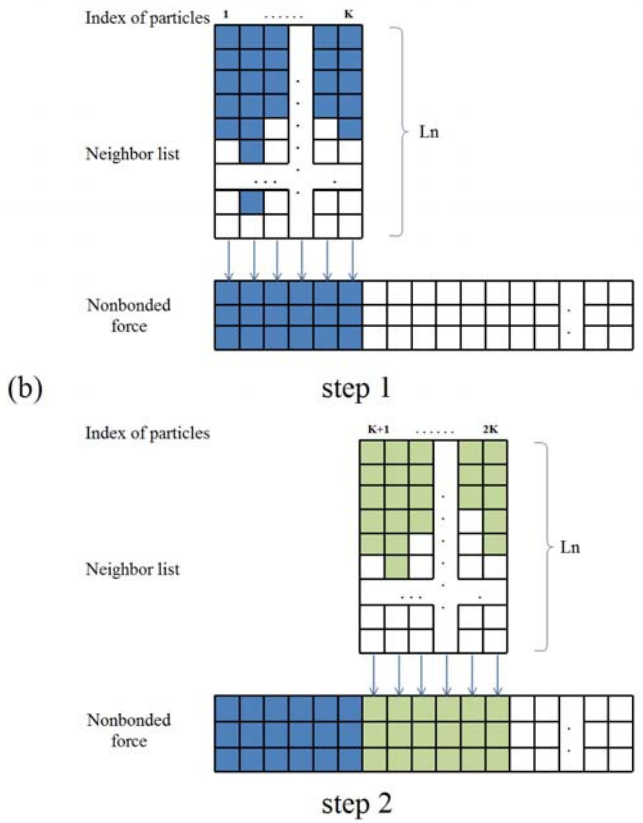

(a)In the normal GPU-based non-bonded force calculations, a complete neighbor list matrix with a fixed size is used.

Tesla C2050 GPU with 3 Gigabyte (GB) device memory

(b) using a novel divide-and-conquer algorithm to reduce the memory requirement

→ Nmax~$1.5*10^7$

Accuracy

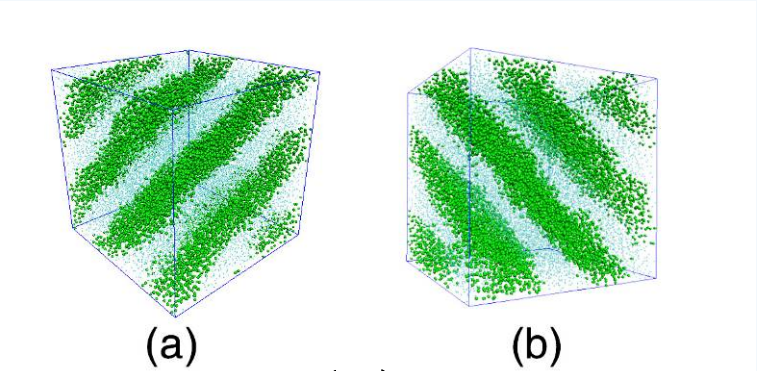

（a） C2050 GPU （b）single E5645 CPU

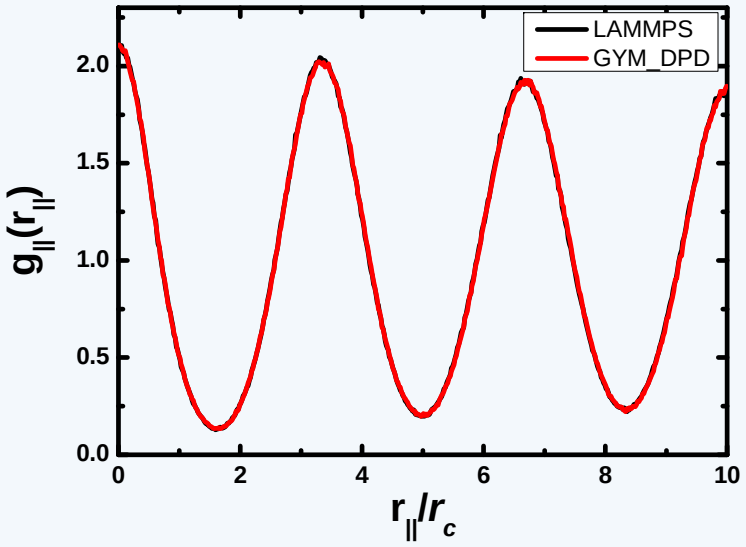

g||(r||) profiles

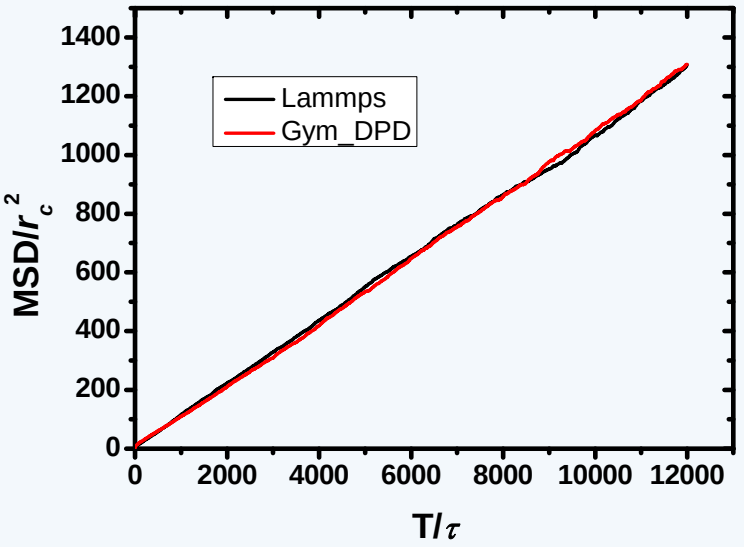

MSD

speedup

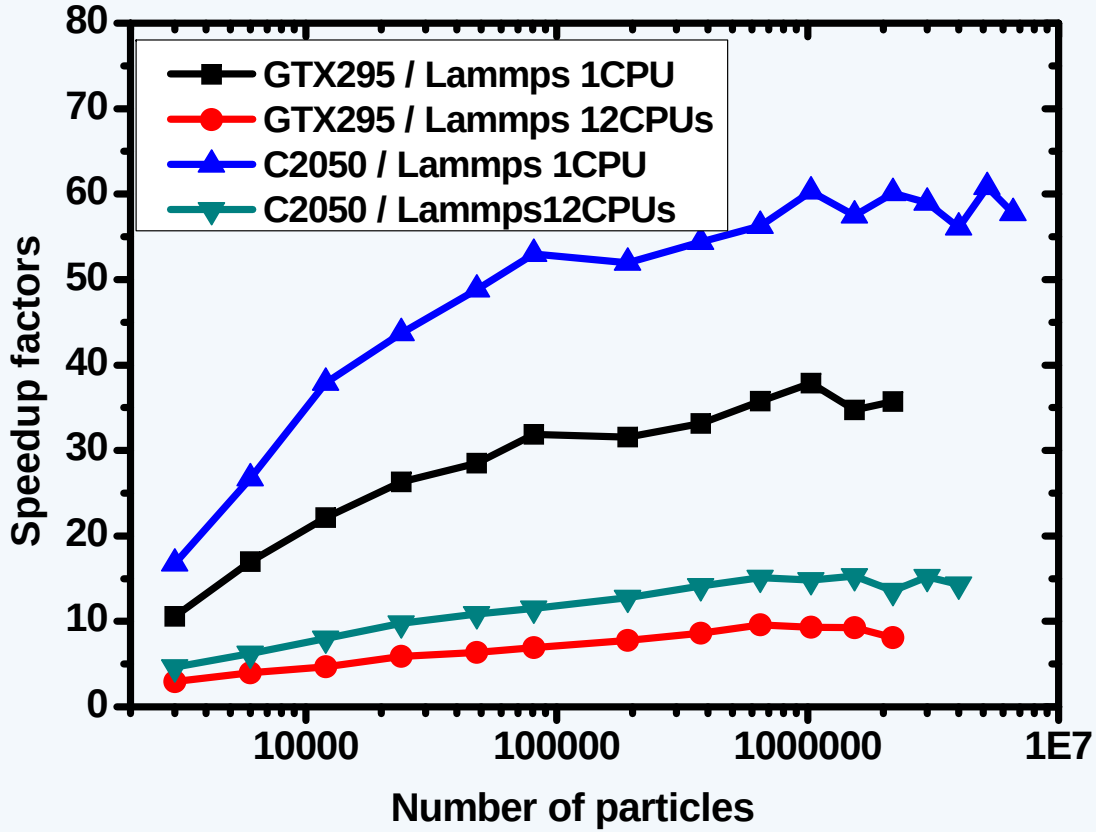
GTX295 / Lammps 1CPU
GTX295 / Lammps 12CPUs
C2050 / Lammps 1CPU
C2050 / Lammps12CPUs
Speedup factors
0
10
20
30
40
50
60
70
80
10000
100000
1000000
1E7
Number of particles

Application:

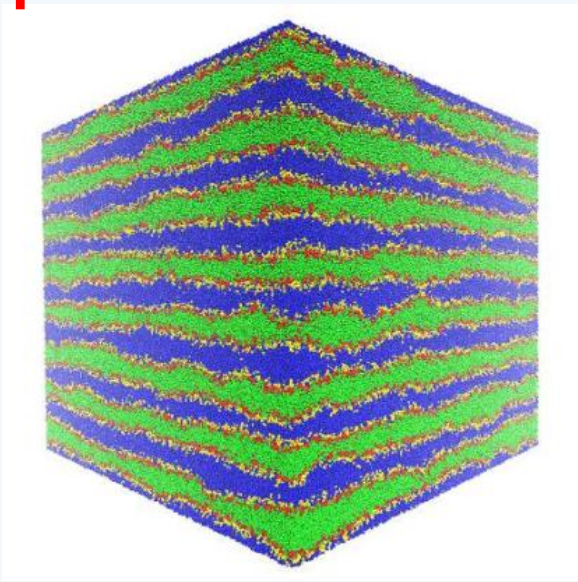

（144*144*160　11, 059, 200 beads）

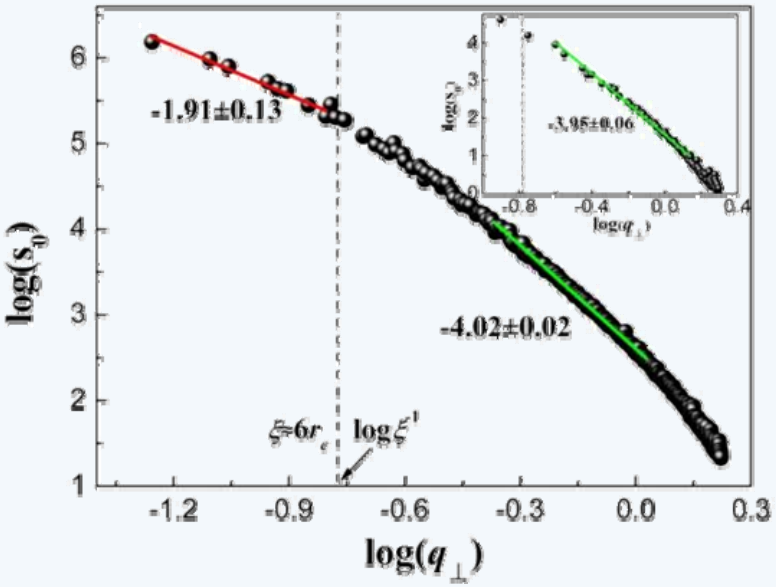

Polymer，54:2146-2157(2013）

1. a complete implementation for the highly efficient and large-scale DPD simulation on a GPU.
2. This implementation is designed and optimized according to the nature of DPD simulation technique and fully takes advantage of the computational power of current GPUs. the GPU-based implementation can predict the results correctly and provide nearly 60 times speedup over LAMMPS on a single Central Processing Unit (CPU) core.

3. using a novel divide-and-conquer algorithm to reduce the memory requirement in simulation, our implementation has the capability to perform large-scale DPD simulations with some ten millions of particles on a single current GPU.

V. Conclusion

- An efficient mesoscopic simulation technique

- An efficient thermostat: local, hydrodynamic conserved, Galilean invariant

Acknowledge

NSFC

ICCAS 1956 中国科学院化学研究所 INSTITUTE OF CHEMISTRY CHINESE ACADEMY OF SCIENCES

Group members:
Dr. Huang, manxia
Dr. Bai, Zhiqiang
Dr. Liu, Xiaohan
Dr. Zhang, Zunmin
Dr. Yang, Keda
Dr. Wu, Shaogui

Thank You

& Questions?